A Distributed Algorithm for Joint Sensing and Routing in Wireless Networks with Non-Steerable Directional Antennas

Chun Zhang[a], Jim Kurose[a], Yong Liu[b], Don Towsley[a], Michael Zink[a]

[a]Dept. of Computer Science,
University of Massachusetts,
Amherst, MA 01003
{czhang, kurose, towsley, zink}@cs.umass.edu

[b]Dept. of Electrical & Computer Engineering
Polytechnic University
Brooklyn, NY 11201
yongliu@poly.edu

Abstract

In many energy-rechargeable wireless sensor networks, sensor nodes must both sense data from the environment, and cooperatively forward sensed data to data sinks. Both data sensing and data forwarding (including data transmission and reception) consume energy at sensor nodes. We present a distributed algorithm for optimal joint allocation of energy between sensing and communication at each node to maximize overall system utility (i.e., the aggregate amount of information received at the data sinks). We consider this problem in the context of wireless sensor networks with directional, non-steerable antennas. We first formulate a joint data-sensing and data-routing optimization problem with both per-node energy-expenditure constraints, and traditional flow routing/conservation constraints. We then simplify this problem by converting it to an equivalent routing problem, and present a distributed gradient-based algorithm that iteratively adjusts the per-node amount of energy allocated between sensing and communication to reach the system-wide optimum. We prove that our algorithm converges to the maximum system utility. We quantitatively demonstrate the energy balance achieved by this algorithm in a network of small, energy-constrained X-band radars, connected via point-to-point 802.11 links with non-steerable directional antennas through numerical simulation.

I. Introduction

Wireless sensor networks have been proposed for myriad applications, ranging from environmental monitoring, to surveillance/security, to industrial control [1]. Sensing and communication are two tasks that must be performed by any such wireless sensor network. The sensing task can be performed either passively (via in-situ observation) or actively (via remote-sensing technologies such as radar, lidar, or sonar), with these latter sensing modalities typically requiring more sensor node resources. Communication can be performed over a variety of wireless radios, ranging from commodity 802.11 (with either longer-distance directional antennas or shorter-distance omni-directional antennas) to specialized mote-based radios. A common requirement of these networks, however, is that they are often energy-constrained, and thus must achieve a balance of how energy is expended among sensing, communication, and computation. This balance needs to be achieved not just locally at an individual node, but *systematically,* since sensor network nodes must interact and collaborate with each other to perform the sensor network's task.

In this paper, we present a distributed algorithm for optimal joint allocation of energy (a resource) between *sensing* and *communication* tasks within a sensor network. To make the problem concrete, we consider a sensing network of collaborating low-powered X-band magnetron radars for meteorological sensing, connected via an 802.11 mesh network with (non-steerable) directional antennas [2]; the energy constraint is imposed by the amount of solar energy that can be harvested and stored from the environment [3]. From a sensing standpoint, we are interested in how much data should be ingested at each individual node, taking into account the amount of energy needed to acquire this data. From the communication standpoint, we are interested in how to route data to a sink, taking into account the energy needed for frame transmission and reception over 802.11 links; note that routing is coupled with link capacity assignment, since, for example, little energy would be needed to provide capacity on a seldomly-used link. The sensing/routing problems are tightly coupled, since it is useless to expend energy acquiring data if there is not sufficient energy to route that data to its destination. The overall objective of the distributed resource allocation algorithm is to maximize the overall sensor network system utility, the aggregate rate at which sensed

information is delivered to sinks. A distributed solution is especially important for wireless sensor networks, given the unpredictable nature of environmental changes, the need to respond to local changes (e.g., in the amount of energy need to realize a given link capacity as a result of environmental changes), and the lack of centralized control.

In this paper, we formulate the sensor network system utility optimization problem as a joint sensing rate control, data routing and energy allocation problem. We first map the combined sensing/routing problem into a unified routing problem [4], using so-called dummy nodes to accommodate the (initially unknown) sensed-data input rates. To solve the resulting two-layer (routing, energy allocation) problem, instead of separating the joint optimization problem into subproblems coordinated by a master dual problem as [5] [6] [7], we use a penalty function approach, in which the virtual costs are directly derived from per-node energy consumption. Our distributed algorithm extends Gallager's distributed routing optimization algorithm for wired networks [8]. In traditional wired network formulations of the resource allocation problem [8] [9] [10], the resource are link-level capacities, with a link's cost increasing as the link-level resource is consumed. In contrast, we consider energy as a node-level resource, with a node energy penalty cost that increases as energy is consumed on a node's incoming links (data sending) and outgoing links (data receiving). By generalizing [8]'s cost function from link-level to node-level, our energy penalty cost function reflects the node-level energy consumption. Our approach to routing also shares similarities with Xue *et al.*'s distributed routing algorithm for wireless networks with given traffic demands [11]. We prove that our generalized distributed algorithm will converge to the optimal system-wide energy allocation between data sensing and data routing. Using our algorithm, we quantitatively demonstrate the energy balance in a network of small, energy-constrained X-band radars, connected via point-to-point 802.11 links with directional antennas via numerical simulation. Our results demonstrate that different nodes in the energy-constrained network should indeed strike a different balance among sensing and communication, e.g., with nodes nearer data sinks expending more energy in communication than nodes near the edge of the sensor network.

Previous work [5] [12] [6] [13] [14] [7] [11] on maximizing network system utility in wireless communication networks do not consider traffic demand generation (i.e., the sensing activity needed to gather and ingest data) as a resource-consuming processes. Assuming that the network system utility is the sum of all data flow utilities, each of which is a concave and increasing function of the flow rate, these works formulate and solve the problem as a convex optimization problem. However, in wireless sensor networks, where the energy used for sensing is not negligible, we demonstrate that energy allocation between both sensing and communication must be considered.

This paper is organized as follows. Section II reviews related work. In section III, we introduce our system model, and formalize the joint data sensing, data routing, and energy allocation problem to maximize the network system utility. In section IV, we map the data sensing, data routing, and energy allocation optimization problem into a data routing, and energy allocation problem. In section V, we present a distributed formulation for this optimization problem. In section VI, we propose our distributed algorithm to solve this problem by generalizing Gallager's result [8]. In section VII, we illustrate the balance achieved between sensing and communication by considering a scenario in which sensor network nodes must balance their energy expenditures among sensing with low-power X-band radars, and communication over point-to-point 802.11 wireless links. In section VIII, we discuss possible extensions and variations to our joint optimization mechanism. We conclude this paper with a summary of this work and some directions for future research.

II. Related Work

The joint rate control, routing and resource allocation problem in wireless networks has been studied by several groups from different angles. Dual decomposition is typically used to separate the joint optimization problem into subproblems, coordinated by a master dual problem, in different ways. In [5], by introducing a price on each *link*, the authors decompose the joint optimization problem into a network flow subproblem, which solves the rate control and routing problems given link prices, and a resource allocation subproblem, which maximizes the network-wide gain. However, no distributed algorithm is developed to solve the two subproblems. In [6], Lin et al., instead, introduced a price on each *node* for forwarding traffic to each destination. The problem is decomposed into a rate control subproblem, and a joint routing and scheduling subproblem. While the rate control subproblem can be solved locally by each node, the routing and scheduling subproblem is solved by a centralized algorithm. The impact of an approximate scheduling algorithm was investigated in [12]. In [7], a similar approach is taken to study the joint

optimization problem with a node-exclusive interference model in which two links sharing a common node cannot transmit or receive simultaneously. Here again, the scheduling problem, essentially a matching problem, is solved in a centralized fashion. A distributed approximate algorithm was presented in the paper. Our approach differs from this earlier work in the following ways: a) we explicitly take into account energy consumption in sensing; b) we consider energy consumption in both data transmission and data reception in wireless networks with non-steerable directional antennas. We develop a fully distributed algorithm to solve the joint sensing rate control, data routing and energy allocation problem; c) instead of adopting the dual decomposition approach, we introduce the notion of a virtual price, derived from an energy consumption penalty function, to directly regulate both sensing and routing. Compared to the dual approach, our approach responds more quickly to environmental changes and avoids energy consumption overflow. Our virtual price approach is similar to the shadow price approach developed in [9] [10] for network rate control. While we use the virtual price to regulate energy allocation on each node, the shadow price in [9] [10] is used to regulate rate allocation on each link. In their setting, each user employs one or multiple fixed routes and determines how much to send to maximize network-wide utility under capacity constraints on all links. In our setting, each node can employ any set of possible routes to reach the sink and tries to maximize network-wide sensing utility under energy constraints on all nodes. The joint scheduling and congestion control problem has also been studied for multi-hop wireless networks in [13] and cellular networks in [14]. They assume user routes are fixed and propose a fair resource allocation consisting of a distributed scheduling algorithm and an asynchronous congestion control algorithm for a node-exclusive interference model.

III. System Model and Problem Formulation

For ease of reading, we list all notations in Table I. We model the wireless sensor network by a directed

TABLE I
NOTATIONS

G	graph	$\odot$	sink
V	$n+1$ node set	$\mathcal{V}$	expanded node set
L	link set	$\mathcal{L}$	expanded link set
$L_I(i)$	links terminate at i	$L_O(i)$	links emanate from i
$L(i)$	$L_I(i) \cup L_O(i)$		
$\mathcal{P}_i$	power budget at i	p_i	power usage at i
P_i^S	sensor-on power at i	p_i^S	sensing power usage
P_{ik}^O	link-on power at i	p_{ik}^O	sending power usage
P_{ik}^I	link-on power at k	p_{ik}^I	receiving power usage
τ_i	sensor-on time fraction	τ_{ik}	link-on time fraction
S_i	sensor-on rate at i	s_i	average sensing rate
$\rho_{ik}F_{ik}$	link-on goodput	f_{ik}	average link goodput
Z	overall power penalty	z_i	power penalty function
D	overall link penalty	d_{ik}	link penalty function
U	utility function	Y	cost function
A	transformed objective		
R_i	traffic initiated $i \rightarrow \odot$	t_i	all traffic $i \rightarrow \odot$
ϕ_{ik}	routing fraction $i \rightarrow k$	η	step size to adjust ϕ
T	period	$\mathcal{E}$	energy budget every T

graph $G = (V, L)$ where V is the set of nodes, and L the set of directed lossy links. Each directed link is implemented by a pair of dedicated radios and non-steerable directional antennas at two end nodes. We assume the data transmission over different links are interference-free. First, we assume that the data transmission over links without common nodes are interference-free due to the fact that directional antenna narrows its beamwidth of the main lobe to the desired direction only. Second, we assume that the data transmission over links with common nodes are interference-free. The interference arising from sidelobes/backlobes can be resolved/mitigated for low-degree network, by placing links with common nodes on non-overlapping/partial-overlapping channels (802.11a offers 12 non-overlapping channels, while 802.11b offers 3) with directional antennas separated by 1 meter [15] [16]. Now we focus on the case where the network has only one data sink. See Section VIII for generalization to multiple sink case. Let $\odot$ denote the single sink node in V, and $1, 2, \ldots, n$ denote non-sink nodes. Let a directional link in

L, from node i to node k, be represented by (i,k). For node i, we let $L_I(i)$ denote the set of links that terminate at node i, and $L_O(i)$ denote the set of links that emanate from i. We denote $L(i) = L_I(i) \cup L_O(i)$ as the set of links adjacent to node i.

Each non-sink sensor node consists of three major components: a sensor, a solar rechargeable battery, and non-steerable directional antennas. We can think of each node operating in a periodic manner. Within each time period T, *(i)* the sensor collects data from its environment, and *(ii)* locally-sensed data and the data the node receives from its upstream neighbors are sent out to its downstream neighbors through directional antennas. To save energy, a sensor/link is assumed to be turned off when no data is being sensed/transmitted. Sensing and data transmission are powered by a solar-rechargeable battery that is continuously charged by a solar panel. In a real environment, a solar panel collects energy at a variable rate. We denote $\mathcal{P}_i$ as the average rate of energy collection over a long time duration, which in turn determines the power supply budget of $\mathcal{P}_i$ for sensing and data communication. (Note: depending on its capacity, the battery can support an instantaneous power consumption rate higher than $\mathcal{P}_i$. The power budget is thus in an average sense and conservatively ensures that the total energy consumption within each period T is bounded by the energy generation. The system is operated in a period manner. For every period T, the energy budget is $\mathcal{E}_i = \mathcal{P}_i T$.

When the sensor of node i is turned on, the data is sensed at fixed rate S_i (referred to as the sensor-on data rate), with fixed power P_i^S consumed at node i (referred to as the sensor-on power). We have,

$$P_i^S = \alpha_i^S S_i \tag{1}$$

where α_i^S is a node-dependent constant.

Sensor of node i is turned on/off to control the amount of sensed data. Let $0 \le \tau_i \le 1$ be the time fraction that the sensor of node i is on for every period T. The average sensing rate at node i, s_i, is

$$s_i = \tau_i S_i \le S_i \tag{2}$$

Within period T, for node i, let p_i^S be the average power allocated for sensing. Combined with equation (1), we have

$$p_i^S = \tau_i P_i^S = \alpha_i^S s_i \tag{3}$$

Each directed link (i,k) is implemented by a pair of non-steerable antennas. When link (i,k) is on, the data is transmitted at fixed raw data rate F_{ik} (referred to as the link-on data rate), with fixed power P_{ik}^O consumed at sender i (referred to as the link-on sender power), and P_{ik}^I consumed at receiver k (referred to as the link-on receiver power). We have,

$$P_{ik}^O = \alpha_{ik}^O F_{ik} \tag{4}$$

$$P_{ik}^I = \alpha_{ik}^I F_{ik} \tag{5}$$

where α_{ik}^O and α_{ik}^I are link-dependent constants. Due to multipath of wireless links, packets may get lost during transmission. We use ρ_{ik} to denote the link (i,k) goodput probability, the link-on goodput of link (i,k) is $\rho_{ik} F_{ik}$.

Link (i,k) is turned off when no data are to be transmitted over the link. Let $0 \le \tau_{ik} \le 1$ be the fraction of time that link (i,k) is on for every period T. The average goodput over link (i,k), f_{ik}, is calculated as follows.

$$f_{ik} = \tau_{ik} \rho_{ik} F_{ik} \le \rho_{ik} F_{ik} \tag{6}$$

At non-sink nodes, flow conservation constraints require that the aggregate outgoing link data rates equal the sum of the incoming data rates (sensing plus incoming transmissions):

$$\sum_{(i,k) \in L_O(i)} f_{ik} - \sum_{(l,i) \in L_I(i)} f_{li} = s_i, \quad i \ne \odot \tag{7}$$

Within period T, for link (i,k), let p_{ik}^O be the average power allocated for transmitting at node i, and p_{ik}^I for receiving at node k. Combined with equations (4)(5), We have,

$$p_{ik}^O = \tau_{ik} P_{ik}^O = \alpha_{ik}^O f_{ik} / \rho_{ik} \tag{8}$$

$$p_{ik}^I = \tau_{ik} P_{ik}^I = \alpha_{ik}^I f_{ik} / \rho_{ik}. \tag{9}$$

Then the average overall power consumption at node i is

$$p_i = p_i^S + \sum_{(l,i)\in L_I(i)} p_{li}^I + \sum_{(i,k)\in L_O(i)} p_{ik}^O \tag{10}$$

Clearly, p_i must be less than or equal to the power budget $\mathcal{P}_i$. Therefore,

$$p_i \le \mathcal{P}_i, \quad i \in V \tag{11}$$

As shown in Figure 1, our goal is to design a joint sensing rate control, data routing, and energy allocation mechanism such that the overall *information* delivered by the wireless sensor network is maximized. We distinguish here between data and information in the following sense. Let s_i be the rate at which sensed data from sensor node i is delivered to the sink $\odot$. A utility function $U_i(s_i)$ quantifies the *value* of this data to the data-consuming applications. We assume that U_i is a concave and increasing function, reflecting the decreasing marginal returns of receiving more data. Our goal is to maximize utility, rather than the rate at which data is delivered.

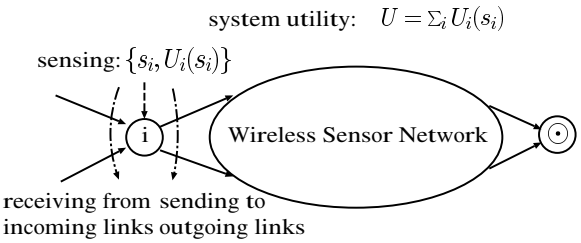

Fig. 1. Maximizing the utility of a wireless sensor network

The joint sensing rate control, data routing and energy allocation problem is then formulated as follows:

Given: $G = (V, L)$, power budget $\mathcal{P}$, sensor/link on-rate S, F and on-power P^S, P^I, P^O, goodput probability ρ
Maximize: network sensing utility $U = \sum_i U_i(s_i)$
Constraints:
1) Flow conservation. See (7).
2) Power constraint. See (11).
3) Sensor/link capacity constraint. See (2)(6).

Given that the utility function U is concave and increasing, the above problem can be solved as a convex optimization problem in a centralized manner. In this paper, we are interested in a distributed solution. We first map the combined sensing/routing problem into a unified routing problem, using so-called dummy nodes to accommodate the (initially unknown) sensed-data input rates. To solve the resulting two-consideration (routing, power allocation) problem, we use a penalty function approach, in which the virtual costs are directly derived from node-level energy utilization. Then we solve the routing/power-allocation problem by generalizing Gallager's distributed algorithm for wired networks [8]. Note that the optimal solution is not affected by the length of the period T. However, as $T \to 0$, the data rates and energy consumption rates are smoothed out to be constant. In practice, it is easier to for intermediate nodes to handle constant flow than bursty flow. In the following, we assume that T is small enough to achieve smoothed data flow rates.

IV. Simplification: from three-considerations to two-considerations

Now we simplify the three-consideration (sensing rate control, data routing, energy allocation) optimization problem defined in III by mapping it to a two-consideration (data routing, energy allocation) optimization problem with fixed traffic demands. We do so by introducing additional dummy nodes, and dummy links as shown in Figure 2.

For each non-sink node $i \in V$, we introduce a dummy node $i' = i + n$. [1] We also add a dummy sensing link (i', i), and a dummy difference link $(i', \odot)$. A fixed-rate traffic demand enters the dummy node i' at rate S_i, which

[1] In this paper, we use i' to denote non-sink node i's corresponding dummy node. i.e., $i' = i + n$

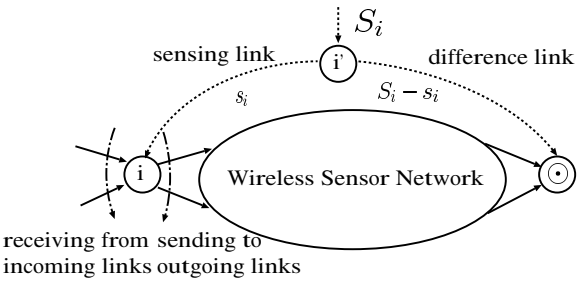

Fig. 2. Mapping from three-layer to two-layer problem

is equal to the maximum achievable sensed data rate of node i. At node i', incoming traffic at rate S_i is forwarded over sensing link (i', i) at rate s_i, or difference link $(i', \odot)$ at rate $S_i - s_i$ towards/to sink $\odot$. The utility to maximize $U = \sum_i U_i(s_i)$ corresponds to utility of data routed over link (i', i). We can equivalently minimize the utility loss over link $(i', \odot)$. i.e., $\min Y = \sum_i Y_i(S_i - s_i)$ where $Y_i(x) = U_i(S_i) - U_i(S_i - x)$. Since the utility function U_i is a concave and increasing function, the cost function Y_i is a convex and increasing function.

We assume that the dummy node i' always has infinite power. i.e.,

$$\mathcal{P}_{i'} = \infty \tag{12}$$

For dummy sensing link (i', i), let the link-on data rate be S_i, the link-on sender power be 0, the link-on receiver power be P_i^S, and the goodput probability be 100%. i.e.,

$$F_{i'i} = S_i, \quad P_{i'i}^O = 0, \quad P_{i'i}^I = P_i^S, \quad \rho_{i'i} = 100\% \tag{13}$$

For dummy difference link $(i', \odot)$, let the link-on data rate be S_i, the link-on sender power be 0, the link-on receiver power be 0, and the goodput probability be 100%. i.e.,

$$F_{i'\odot} = S_i, \quad P_{i'\odot}^O = 0, \quad P_{i'\odot}^I = 0, \quad \rho_{i'\odot} = 100\% \tag{14}$$

The sensing rate at node i, s_i, then corresponds to the goodput rate over link (i', i), $f_{i'i}$, where

$$f_{i'i} = \tau_{i'i} F_{i'i} \tag{15}$$

where $\tau_{i'i}$ is the fraction of time that dummy sensing link (i', i) is on.

We now formally map the original three-consideration optimization problem into a joint data routing and resource allocation problem with fixed traffic demands. Let $\mathcal{V} = \{\odot, 1, ..., n, n+1, ..., 2n\}$ denote the expanded node sets, and $\mathcal{L} = L \cup \{(i', i), (i', \odot) | i \in V - \{\odot\}\}$ the expanded link sets. We use $R = \{R_1, \ldots, R_{2n}\}$ to denote the traffic demand, where R_i is the average data rate originated from node i destined to sink $\odot$. We have,

$$R_i = 0, \quad i \in \{\odot, 1, ..., n\} \tag{16}$$

$$R_{i'} = S_i, \quad i' \in \{n+1, ..., 2n\} \tag{17}$$

Given fixed traffic demand R, the flow conservation constraint is expressed:

$$\sum_{(i,k) \in L_O(i)} f_{ik} - \sum_{(l,i) \in L_I(i)} f_{li} = R_i, \quad i \neq \odot \tag{18}$$

We use p_i to denote the node i overall power consumption. Since there is no sensing operation, we have

$$p_i = \sum_{(l,i) \in L_I(i)} p_{li}^I + \sum_{(i,k) \in L_O(i)} p_{ik}^O \tag{19}$$

It is straightforward to see that the joint sensing rate control, data routing, and energy allocation problem defined in Section III is equivalent to the joint data routing and energy allocation problem defined as follows:

Given: network $\mathcal{G} = (\mathcal{V}, \mathcal{L})$, power budget $\mathcal{P}$, link on-rate F and on-power P^I, P^O, goodput probability ρ, fixed demand R
Minimize: Cost $Y = \sum_{(i',\odot)\in\mathcal{L}} Y_i(f_{i'\odot})$.
Constraints:
1) Flow conservation. See (18).
2) Power constraint. See (11).
3) Link capacity constraint. See (6).

In this paper, we introduce convex and increasing penalty functions to replace the power constraints, and link capacity constraints. We use power penalty functions $z_i(p_i)$ at each node $i \in \{1, \ldots, n\}$ to replace power constraints; and link capacity penalty functions $d_{ik}(f_{ik})$ at each link $(i,k) \in L$ to replace link capacity constraints. We have,

$$\lim_{p_i \to P_i} z_i(p_i) \to \infty, \quad \{1, \ldots, n\} \tag{20}$$

$$\lim_{f_{ik} \to \rho_{ik} F_{ik}} d_{ik}(f_{ik}) \to \infty, \quad (i,k) \in L \tag{21}$$

Let $D + Z = \sum_{(i,k)\in L} d_{ik}(f_{ik}) + \sum_{i\in\{1,\ldots,n\}} z_i(p_i)$ be the network overall penalty cost. Then the problem becomes:

Given: network $\mathcal{G} = (\mathcal{V}, \mathcal{L})$, power budget $\mathcal{P}$, link on-rate F and on-power P^I, P^O, fixed demand R
Minimize: Cost $A = Y + D + Z$.
Constraints: Flow conservation. See (18).

In order to design a distributed algorithm, we further decompose cost A into node-level local costs. The node i cost, A_i, is defined as follows.

$$\begin{aligned} A_i &= z_i(p_i) + \sum_{(i,k)\in L_O(i)} d_{ik}(f_{ik}), \quad i \in \{1, \ldots, n\} \\ A_i &= Y_{iw}(f_{iw}), \quad i \in \{n+1, \ldots, 2n\} \end{aligned} \tag{22}$$

Therefore,

$$A = \sum_{i\in\mathcal{V}} A_i \tag{23}$$

The use of penalty function can result in an allocation that is not strictly identical to the optimal solution to the original problem before the penalty function was introduced. However, this standard approach typically results in a solution that is nearly the optimal solution to the initial problem formulation [17]. A penalty function may also prevent a node energy (or a link capacity) from being completely allocated. In practice, such remaining energy (or capacity) could be used to better accommodate the changing demand, or be used for faster recovery in the case of node or link failures.

V. Distributed Problem Formulation for Joint Routing and Energy Allocation

In the previous section, the joint routing and energy allocation problem formulation used flow rates f as the optimization control variables. However, these flow rates f are global information. In order to solve this problem using a distributed algorithm, we reformulate the problem using local routing fractions as control variables.

Let t_i be the total expected traffic rate at node $i \in \mathcal{V}$. Thus t_i includes both R_i and traffic from other nodes that is routed through i. Let ϕ_{ik} be the fraction of t_i that is routed over link (i,k). Since t_i is the sum of the data rate entering the network at i and the traffic routed to i from other nodes,

$$t_i = R_i + \sum_l t_l \phi_{li} \tag{24}$$

$$f_{ik} = t_i \phi_{ik} \tag{25}$$

Equation (24) implicitly expresses the conservation of flow at each node: the traffic rate into a node for sink $\odot$ is equal to the traffic rate out of the node for sink $\odot$. Next, we define ϕ the same ways as [8] to ensure that equation (24) has a unique solution of t given R and ϕ.

Definition : A routing variable set ϕ for network $\mathcal{G} = (\mathcal{V}, \mathcal{L})$ with sink node $\odot$ is a set of nonnegative numbers ϕ_{ik}, $i, k \in \mathcal{V}$, satisfying the following conditions.

1) $\phi_{ik} = 0$ if $i = \odot$, or $(i, k) \notin \mathcal{L}$,
2) $\sum_k \phi_{ik} = 1$ if $i \neq \odot$,
3) $\forall i \neq \odot$, there is a routing path from i to $\odot$, which means there is a sequence of nodes, $i, k, l, \ldots, m$ such that $\phi_{ik} > 0$, $\phi_{kl} > 0$, $\ldots$, $\phi_{m\odot} > 0$.

Theorem 5.1: Let a network $\mathcal{G} = (\mathcal{V}, \mathcal{L})$ have input set R and routing variable set ϕ. Then the set of equations (24) has a unique solution for t. Each component t_i is nonnegative and continuously differentiable as a function of R and ϕ.

Proof: Proved in [8]. Included in Appendix A for completeness. ■

The joint data routing and energy allocation problem is reformulated using routing variable Φ as control variables:

Given: network $\mathcal{G} = (\mathcal{V}, \mathcal{L})$, power budget $\mathcal{P}$, link on-rate F and on-power P^I, P^O, fixed demand R
Minimize: Cost $A = \sum_i A_i$.
Constraints: Flow set f is implemented by routing variable set ϕ.

Next, we propose a distributed algorithm to solve the above problem. In this algorithm, each node makes its own local energy allocation decision and constructs its own routing tables based on periodic update information from its neighbors.

VI. Distributed Algorithm for Joint Routing and Energy Allocation

Now we solve the joint routing and energy allocation optimization problem by generalizing Gallager's distributed algorithm [8]. We note that while Gallagers algorithms need only consider the rate of flows at *link-level* (due to its assumption of a wired network, and the goal of minimizing delay), in wireless networks, we must further consider both incoming and outgoing links at *node-level*, since node energy is expended in both sending and receiving packets. We first solve this optimization problem in the case of fixed routing (thus fixed data flow). With a fixed set of routes, the energy allocation problem is then decoupled so that each node independently allocates energy to satisfy the data flow. In addition, each node also locally calculates the marginal cost with respect to link data rates. These marginal cost then drive the global routing optimization similar in spirit to [8].

A. Power Allocation for Fixed Data Flow f

With fixed route set ϕ (thus fixed f), each node i requires power $p^O_{ik}(f_{ik})$ on outgoing link (i, k) for data transmission, and power $p^I_{li}(f_{li})$ on incoming link (l, i) for data reception. From equations $(6)(8)(9)$, power allocation p_i is determined by flow rates f (or data routing ϕ). Combined with equation (22), the objective function A to minimize can be viewed solely as a function of flow rates f (or routing variables ϕ). Next, we use $A^f(f) = \sum_i A^f_i(f)$ (or $A^\phi(\phi)$) to denote A as a function of f (or ϕ).

While optimizing energy to satisfy a fixed data flow f, each node i also locally calculates the marginal cost with respect to the link data rates $\partial A^f_i(f)/\partial f_{kl}$, $(k, l) \in L(i)$. An increase of data flow f_{kl} requires a concomitant increase of energy consumption at both sender node i and receiver node j, which results in the increase of cost at both sender node i and receiver node j. Therefore, the marginal global cost with respect to the link data rate of link (k, l), $\partial A^f(f)/\partial f_{kl}$, is calculated as the sum of marginal node cost over two end nodes k and l.

$$\frac{\partial A^f(f)}{\partial f_{kl}} = \frac{\partial A^f_k(f)}{\partial f_{kl}} + \frac{\partial A^f_l(f)}{\partial f_{kl}} \tag{26}$$

Note that these marginal global costs $\partial A^f(f)/\partial f_{kl}$ can be derived through local communication between nodes k and l.

Next, we focus on distributed routing optimization. i.e., an algorithm for each node to locally adjust routing variables to converge to the optimal set of routes by generalizing Gallager's result [8]. We first generalize [8]'s necessary and sufficient condition for optimal set of routes.

B. Necessary and Sufficient Conditions for Optimal Cost

Now we generalize [8]'s necessary and sufficient conditions to minimize A^ϕ over all feasible sets of routes. Similar to [8], we compute the partial derivatives of A^ϕ with respect to the inputs R and the routing variables ϕ as follows.

$$\frac{\partial A^\phi(\phi)}{\partial R_i} = \sum_k \phi_{ik} \left[\frac{\partial A^f(f)}{\partial f_{ik}} + \frac{\partial A^\phi(\phi)}{\partial R_k} \right] \tag{27}$$

$$\frac{\partial A^\phi(\phi)}{\partial \phi_{ik}} = t_i \left[\frac{\partial A^f(f)}{\partial f_{ik}} + \frac{\partial A^\phi(\phi)}{\partial R_k} \right] \tag{28}$$

The existence and uniqueness of $\partial A^\phi(\phi)/\partial R_i$ and $\partial A^\phi(\phi)/\partial \phi_{ik}$ is given by the following theorem.

Theorem 6.1: Let a network $\mathcal{G} = (\mathcal{V}, \mathcal{L})$ have input traffic set R and routing variable set ϕ, and let each marginal link cost $\frac{\partial A^f(f)}{\partial f_{ik}}$ be continuous in $f_{ik}, (i,k) \in \mathcal{L}$. Then the set of equations (27) has a unique set of solutions for $\frac{\partial A^\phi(\phi)}{\partial R_i}$. Furthermore, (28) is valid and both $\frac{\partial A^\phi(\phi)}{\partial R_i}$ and $\frac{\partial A^\phi(\phi)}{\partial \phi_{ik}}$ for $(i,k) \in \mathcal{L}$ are continuous in R and ϕ.

Proof: See Appendix B. ■

Using Lagrange multipliers for the constraint $\sum_k \phi_{ik} = 1$, and taking into account the constraint $\phi_{ik} \geq 0$, the necessary conditions with respect to ϕ are, $(i,k) \in \mathcal{L}$,

$$\frac{\partial A^\phi(\phi)}{\partial \phi_{ik}} \begin{cases} = \lambda_i & \phi_{ik} > 0 \\ \geq \lambda_i & \phi_{ik} = 0. \end{cases} \tag{29}$$

However, as shown by [8], (29) is not a sufficient condition to minimize A^ϕ even for the routing optimization problem in wired networks. Next, we proceed to show the sufficient condition for the optimization problem.

Theorem 6.2: Let $\mathcal{F}$ be a convex and compact set of flow sets, which is enclosed by $|\mathcal{L}|$ planes (each of which corresponds to $f_{ik} = 0$, $(i,k) \in \mathcal{L}$), and a boundary envelope $\mathcal{F}_\infty$. Assume that A^f is convex and continuously differentiable for $f \in \mathcal{F} - \mathcal{F}_\infty$, Let Ψ be the set of ϕ for which the resulting set of flow rates f are in the above convex and bounded set $\mathcal{F} - \mathcal{F}_\infty$. Then (30) is sufficient to minimize A^ϕ over Ψ, for all $(i,k) \in \mathcal{L}$

$$\frac{\partial A^f(f)}{\partial f_{ik}} + \frac{\partial A^\phi(\phi)}{\partial R_k} \geq \frac{\partial A^\phi(\phi)}{\partial R_i} \tag{30}$$

Proof: See Appendix C. ■

C. A Distributed Algorithm for Routing Optimization

Based on the above sufficient condition, we now develop a gradient-based algorithm by generalizing [8]. Each node i must incrementally decrease those routing variables ϕ_{ik} for which the marginal cost $\partial A^f(f)/\partial f_{ik} + \partial A^\phi(\phi)/\partial R_k$ is large, and increase those for which it is small. The algorithm breaks into two parts: a protocol between nodes to calculate the marginal costs, and an algorithm for calculating the routing updates and modifying the routing variables.

Given goodput rates f_{kl} for each incoming and outgoing link $(k,l) \in L(i)$, each node i locally allocates power to satisfy the traffic, and calculates $\partial A_i^f(f)/\partial f_{kl}, (k,l) \in L(i)$. Then, for each pair of neighbor node i, j with common link (i,j), node j sends $\partial A_j^f(f)/\partial f_{ij}$ to node i. Upon receiving it from node j, node i computes $\partial A^f(f)/\partial f_{ij}$ using (26).

In order to see how node i can calculate $\partial A^\phi(\phi)/\partial R_i$. Define node m to be downstream from node i (with respect to sink node $\odot$) if there is a routing path from i to $\odot$ passing through m (i.e., a path with positive routing variables on each link). Similarly, we define i as upstream from m if m is downstream from i. A routing variable set ϕ is loop free if there is no i, m $(i \neq m)$ such that i is both upstream and downstream for m. The protocol used for an update, now, is as follows: each node i waits until it has received the value $\partial A^\phi(\phi)/\partial R_k$ from each of its downstream neighbors $k \neq \odot$. The node i then calculates $\partial A^\phi(\phi)/\partial R_i$ from (27) (using the convention that $\partial A^\phi(\phi)/\partial R_\odot = 0$) and broadcasts this to all of its neighbors. It is easy to see that this procedure is free of deadlocks if and only if ϕ is loop-free.

To avoid deadlocks, our algorithm requires a small amount of additional information to maintain loop-free property: each node i maintains a set B_i of blocked node k for which $\phi_{ik} = 0$ and the algorithm is not permitted to increase ϕ_{ik} from 0. Next, we first introduce the algorithm, and then define B more accurately.

The algorithm Γ, on each iteration, maps the current routing variable ϕ into a new set $\phi^1 = \Gamma(\phi)$. The mapping is defined as follows. For $k \in B_i$,

$$\phi^1_{ik} = 0, \quad \Delta_{ik} = 0. \tag{31}$$

For $k \notin B_i$, define

$$a_{ik} = \frac{\partial A^f(f)}{\partial f_{ik}} + \frac{\partial A^\phi(\phi)}{\partial R_k} - \min_{m \notin B_i} \left[\frac{\partial A^f(f)}{\partial f_{im}} + \frac{\partial A^\phi(\phi)}{\partial R_m} \right] \tag{32}$$

$$\Delta_{ik} = \min[\phi_{ik}, \eta a_{ik}/t_i] \tag{33}$$

where η is a scale parameter of Γ to be discussed later. Let $k_{min}(i,j)$ be a value of m that achieves the minimization in (33). Then

$$\phi^1_{ik} = \begin{cases} \phi_{ik} - \Delta_{ik} & k \neq k_{min}(i,j) \\ \phi_{ik} + \sum_{k \neq k_{min}(i,j)} \Delta_{ik} & k = k_{min}(i,j). \end{cases} \tag{34}$$

The algorithm reduces the fraction of traffic (and thus energy) sent on non-optimal links and increases the fraction on the best link. The amount of reduction, given by Δ_{ik}, is proportional to a_{ik}, with the restriction that ϕ^1_{ik} cannot be negative. In turn a_{ik} is the difference between the marginal cost to sink $\odot$ using link (i,k) and using the best link. Note that as the sufficient condition (30) is approached, the changes get small, as desired. The amount of reduction is also inversely proportional to t_i. The reason for this is that the change in link traffic is related to $\Delta_{ik} t_i$. Thus when t_i is small, Δ_{ik} can be changed by a large amount without greatly affecting the marginal cost. Finally the changes depend on the scale factor η. For η very small, convergence of the algorithm is guaranteed, as shown in Theorem 6.4, but rather slow. As η increases, the speed of convergence increases but the danger of no convergence increases.

We now complete the definition of algorithm Γ by defining the block sets B_i. See [8] for further reasoning on how this definition guarantees the loop-free property.

First define a routing variable ϕ_{ik} to be *improper* if $\phi_{ik} > 0$ and $\partial A^\phi(\phi)/\partial R_i \leq \partial A^\phi(\phi)/\partial R_k$. We have already said that B_i includes only k for which $\phi_{ik} = 0$, and thus, from (27),

$$\min_{m \notin B_i} \frac{\partial A^f(f)}{\partial f_{im}} + \frac{\partial A^\phi(\phi)}{\partial R_m} \leq \frac{\partial A^\phi(\phi)}{\partial R_i} \tag{35}$$

Assuming positive marginal costs, $\partial A^\phi(\phi)/\partial R_i < \partial A^f(f)/\partial f_{ik} + \partial A^\phi(\phi)/\partial R_k$ if ϕ_{ik} is improper, and we see that the algorithm always reduces improper routing variables. In fact, since $\partial A^\phi(\phi)/\partial R_i$ is the marginal cost for the traffic originating from i to $\odot$, we would expect marginal cost to decrease as we move downstream, and improper routing variables should be rather atypical. Note that if there are no improper routing variables, the set of marginal costs $\partial A^\phi(\phi) \partial R_i$ would form an partial ordering of the nodes i. Similar to [8], if ϕ is loop-free and $\phi^1 = \Gamma(\phi)$ contains a loop, then the following two conditions must hold.

1) The loop contains some link (i,k) for which $\phi_{ik} = 0$, $\phi^1_{ik} > 0$, and $\partial A^\phi(\phi)/\partial R_i > \partial A^\phi(\phi)/\partial R_k$.
2) The loop contains some link (l,m) for which ϕ_{lm} is improper and for which $\phi^1_{lm} > 0$.

The first condition reiterates that some routing variables must be increased from 0 to form a loop and that the algorithm only increases routing variables on links to nodes with smaller marginal cost. The second make use of the fact that if nodes are ranked by marginal cost, $\partial A^\phi(\phi)/\partial R_i$, then it is impossible to move around a loop of nodes and have marginal cost monotonically decrease.

Definition: The set B_k is the set of nodes k for which both $\phi_{ik} = 0$ and k is blocked. A node k is blocked if k has a routing path to sink $\odot$ containing some link (l,m) for which $\phi_{lm} > 0$, and $\partial A^\phi(\phi)/\partial R_l \leq \partial A^\phi(\phi)/\partial R_m$, and

$$\phi_{lm} \geq \eta \left[\frac{\partial A^f(f)}{\partial f_{lm}} + \frac{\partial A^\phi(\phi)}{\partial R_m} - \frac{\partial A^\phi(\phi)}{\partial R_l} \right] \Big/ t_i \tag{36}$$

Theorem 6.3: If the marginal link costs $\partial A^f(f)/\partial f_{lm}$ are positive and ϕ is loop-free, then $\phi^1 = A(\phi)$ is loop-free.

Proof: Following similar proof in [8]. ■

The protocol required for a node i to determine the set B_i is as follows. Each node l, when it calculates $\partial A^\phi(\phi)/\partial R_l$, determines, for each downstream m, if $\phi_{lm} > 0$, and $\partial A^\phi(\phi)/\partial R_l \leq \partial A^\phi(\phi)/\partial R_m$, and satisfy (36). If any downstream neighbor satisfies these conditions, node l adds a special tag to its broadcast of $\partial A^\phi(\phi)/\partial R_l$. The node l also adds the special tag if the received value $\partial A^\phi(\phi)/\partial R_m$ from any downstream m contained a tag. In this way all nodes upstream of l also send the tag. The set B_i is then the set of nodes k for which the received $\partial A^\phi(\phi)/\partial R_k$ was tagged.

Theorem 6.4: Let $\mathcal{F}$ be a convex and compact set of flow sets, which is enclosed by $|\mathcal{L}|$ planes (each of which corresponds to $f_{ij} = 0$, $(i,j) \in \mathcal{L}$), and a boundary envelope $\mathcal{F}_\infty$. Assume that A^f is a convex and increasing function for $f \in \mathcal{F} - \mathcal{F}_\infty$ and that $\forall f_\infty \in F_\infty$, $\lim_{f \to f_\infty^-} A^f = \infty$. For every positive number A^0, if ϕ^0 satisfies $A^\phi(\phi^0) \leq A^0$, then with scale factor $\eta = [M|\mathcal{V}|^7]^{-1}$,

$$\lim_{m\to\infty} \Gamma(\phi^m) = \min_{\phi}(A^\phi(\phi)) \tag{37}$$

where

$$M = \max_{(l_1,m_1),(l_2,m_2)\in\mathcal{L}} \max_{f:A^f(f)\leq A^0} \frac{\partial^2 A^f(f)}{\partial f_{l_1m_1}\partial f_{l_2m_2}} \tag{38}$$

Proof: See Appendix D. ■

Compared with result from Gallager's work [8], our work requires smaller η to guarantee convergence because we consider more general problem definition than [8]. The proof uses a ridiculously small value of η to guarantee convergence under all conditions. In next section, we use simulation to identify practical values for η.

We have proposed a distributed algorithm for routing optimization. Note that in each iteration, the power allocation achieves optimality through local independent local power allocation. Combining the collective routing optimization, and independent local power allocation at all nodes, we have achieved the optimal cost over all feasible resource allocation and routing combinations.

D. Mapping solution back to three-consideration optimization problem

The optimal solution of the two-consideration (data routing, energy allocation) optimization problem can be easily mapped back to the optimal solution of the three-consideration (data sensing, data routing, and energy allocation) optimization problem as follows.

First, for each node i, the optimal average sensing rate s_i is equal to $f_{i'i}$. Therefore,

$$s_i = f_{i'i}, \quad p_i^S = \alpha_i^S f_{i'i}, \quad \tau_i = s_i/S_i \tag{39}$$

Second, for each link (i,k), the optimal average goodput rate f_{ik} is directly derived from optimization result. Therefore,

$$\tau_{ik} = \frac{f_{ik}}{\rho_{ik}F_{ik}} \tag{40}$$

Finally, the routing fraction ϕ_{ik} is directly derived from two-consideration optimization results. We have mapped the two-consideration solution back to three-consideration solution.

VII. RESULT

In this section we examine the optimal solution of the joint sensing and routing problem. We first focus on energy rich networks, then energy constrained networks.

A. Energy rich wireless sensor networks

As a special case of wireless sensor networks, energy rich network is not energy constrained: it either has direct power supply, or good energy harvest source. For energy rich network, we show that if all nodes use the same utility function, the optimal sensing rates is max-min fair.

Theorem 7.1: For an energy rich sensor network $G = (V, E)$ with a single sink, all nodes use the same utility function. i.e., $U_i = U_j \ \forall i, j \in V$. If the utility function is strictly concave, the optimal sensing rates s^* (of problem defined in section III) satisfy max-min fairness.

Proof: Since there is no energy constraints in energy-rich wireless sensor networks, link capacity can be fully implemented as link-on goodput rate. In the following proof, we use link capacity and link-on goodput rate interchangeably.

Let s^* be the optimal sensing rate allocation, and x be the sorted order of nodes such that $\forall k \in \{1, \ldots, n-1\}$, $s^*_{x_k} \leq s^*_{x_{k+1}}$.

If $\forall k \in \{1, \ldots, n-1\}$, $s^*_{x_k} = s^*_{x_{k+1}}$, then s^* is max-min fairness.

Otherwise, $\exists k \in \{1, \ldots, n-1\}$, $s^*_{x_k} < s^*_{x_{k+1}}$. We further prove the theorem through three steps.

Step 1, if $s^*_{x_i} < s^*_{x_j}$, then node x_i doesn't forward traffic injected from node x_j.

Otherwise, $\{\ldots, s^*_{x_i} + \delta, \ldots, s^*_{x_j} - \delta, \ldots\}$ would be a feasible and better solution where δ is an arbitrary small amount of traffic.

Step 2, if $s^*_{x_k} < s^*_{x_{k+1}}$ or $k = n$, then $\sum_{i \leq k} s^*_{x_i} = C_k$ where C_k is the minimum cut of graph G_k, which is constructed as follows: given graph G with sink $\odot$, we add a virtual source $\mathcal{S}$. Then we add links between virtual source node $\mathcal{S}$, and x_i ($\forall i \leq k$). The link-on goodput rate of link $(\mathcal{S}, x_i)$ is set to be ∞. C_k refers to the minimum cut of graph G_k between the virtual source $\mathcal{S}$ and sink $\odot$. Because C_k is the min cut between virtual source $\mathcal{S}$ and sink $\odot$, we have $\sum_{i \leq k} s^*_{x_i} \leq C_k$. If $\sum_{i \leq k} s^*_{x_i} < C_k$, then there exists an augmenting path in graph C_k: $\mathcal{S}, x_j, \ldots, \odot$, $j \leq k$. If all links on the augmenting path do not include any traffic from node x_l, $l > k$, then one can increase x^*_j by δ and get a better solution $\{\ldots, s^*_{x_j} + \delta, \ldots\}$. Contradiction! Otherwise, the augmenting path must include a link carrying traffic from some node x_l where $l > k$. Let node m be the first node on the augmenting path forwarding traffic for node x_l ($l > k$). As the augmenting path has reached node m, it is enough to increase j's traffic by reducing traffic carried by node m for node l. Again, $\{\ldots, s^*_{x_j} + \delta, \ldots, s^*_{x_l} - \delta, \ldots\}$ will be a feasible and better solution. Contradiction!

Step 3, $\{s^*_i\}$ is max-min fair. Since $\forall k \in \{1, \ldots, n-1\}$, if $s^*_{x_k} < s^*_{x_{k+1}}$, then $\sum_{i \leq k} s^*_{x_i} = C_k$, as well as $\forall k \in \{1, \ldots, n-1\}$, $s^*_{x_k} \leq s^*_{x_{k+1}}$, one cannot increase $s^*_{x_k}$ without decreasing $s^*_{x_j}$, $j < k$.

■

Due to the uniqueness of max-min fair sensing rates [18], Theorem 7.1 also suggests that the optimal sensing rates are independent of choice of utility function. Moreover, efficient algorithms [19] exist to find the max-min fair solution.

However, as we identified in this paper, Theorem 7.1 generally does not hold for energy constrained networks. Next, we demonstrate this via a simple counter example. In this example, we use a three-node network shown in Figure 3.

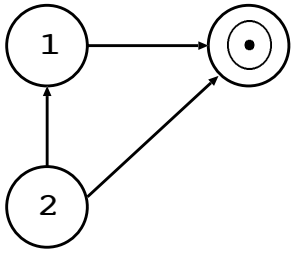

Fig. 3. A topology to illustrate that optimal sensing rates are not max-min fair for energy constrained wireless sensor networks

In this example, both node 1 and node 2 have a power budget of $\mathcal{P}_1 = \mathcal{P}_2 = 1W$. For simplicity, we assume that only data sending consumes energy, while data receiving and data sensing consumes no energy. We also assume data transmission is loss-free. The link-on goodput rates of all links are $1Mbps$. However, the energy used per unit traffic are different. $\alpha^O_{1,\odot} = 1W/Mbps$, $\alpha^O_{2,\odot} = 2.5W/Mbps$, $\alpha^O_{2,1} = 2W/Mbps$. Clearly, the max-min fair solution is $(s_1, s_2) = (0.5Mbps, 0.5Mbps)$. However, $(s_1, s_2) = (1Mpbs, 0.4Mpbs)$ is a better solution when node 1 and

node 2 uses the same concave utility function $\log(x+1)$. Therefore, the optimal sensing rates must not be max-min fair in this case.

We have seen that Theorem 7.1 generally does not hold for energy constrained networks. Next, we further examine the optimal solution for energy constrained networks through numerical simulations.

B. Energy constrained wireless sensor networks

We examine the optimal sensing rates through numerical simulation using parameters derived from an on-going weather-monitoring project [2]. Our numerical simulator use the model and the optimization algorithm as described in previous sections. In the simulation scenario in Figure 4, we consider a wireless sensor network composed of 30 collaborating lower-powered X-band magnetron radars for meteorological sensing, connected via an 802.11b mesh network with non-steerable directional antennas. All sensed data are destined to sink $\odot$. Each link is implemented by a pair of radios and directional antennas at the sender and the receiver. Note that between each pair of neighboring nodes, we only need one pair of directional antennas because of the loop free property of optimal routing solution: data can only fly in one direction at one time. To reduce the interference, we use four partial-overlapping channels $(1, 4, 8, 11)$ (marked as A, B, C, D in Figure 4): links on straight line reuse the same channel every 4 hops; links sharing the same sensor node are assigned to different channels. To further reduce the interference, at each node, we physically separate the radios and antennas on different channels by 1 meter. For sink node, we physically separate the distance between antenna $(6, \odot)$ and $(30, \odot)$ by 100 meters.

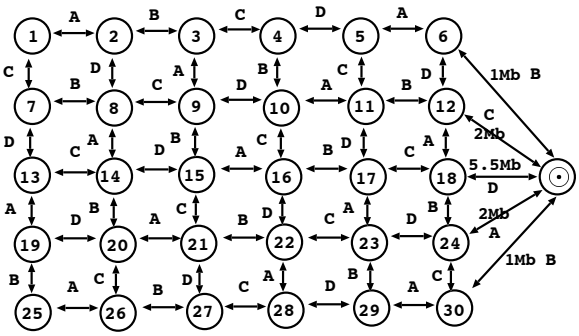

Fig. 4. Topology used for Simulation

When a sensing radar is on, its power consumption is $p_i^S = 34$W (based on a RayMarine 24 inch, 4kW radar), generating sensed data at rate $S_i = 1.5Mbps$. When a link is on, the power consumption at the sender is $P_i^O = 1.98W$, and $P_i^I = 1.39W$ at the receiver. The link-on data rate is determined by distance between two end nodes. Based on our preliminary measurement, the link-on goodput rate for links $(6, \odot)$ and $(30, \odot)$ are, $\rho_{6,\odot}F_{6,\odot} = \rho_{30,\odot}F_{30,\odot} = 1Mbps$; the link-on goodput rate for link $(18, \odot)$ is, $\rho_{18,\odot}F_{18,\odot} = 5.5Mbps$. For all other links (i, k), $\rho_{ik}F_{ik} = 2Mbps$.

A solar-rechargeable battery is used for power. The energy charging process is affected by weather. During a sunny day, the energy collected per day is measured at $312Wh$, which translates to a power budget $\mathcal{P}_i = 13W$. During the cloudy day, the energy collected per day is measured at $168Wh$, which translates to $\mathcal{P}_i = 7W$. The battery capacity is $110Ah$, for $12V$ operation, it can store energy $1230Wh$, that relates to 94 hours if the power is consumed at $13W$. We prefer a smoothed energy usage: every 24 hours, we recompute the power budget $\mathcal{P}_i$ based on the overall energy in the battery: $\mathcal{P}_i$ is set to be the overall energy in the battery at that time divided by 48 hours. By doing so, the energy consumption rate is smoothed over a window size of 48 hours.

We use the negative standard error of the environment's reflectivity estimate σ_i as the node i utilization function [20].

$$U_i(s_i) = -\omega_i s_i^{-0.5} \tag{41}$$

in which ω_i is the weight of utility at node i.

Next, we first present numerical results of our distributed algorithm in the synthetic wireless network described above. We will illustrate how the choice of step-size scale factor η affects convergence speed. It will become clear that, in practice, it is possible to choose a η much larger than the value used in the proof of Theorem 6.4 to expedite

the convergence. Second, through optimization over different power budgets, we demonstrate how the power budget affects the energy allocation decision between data sensing and data communication.

1) Scale factor η and convergence: In the previous section, with a small scale factor η, we have shown that optimization algorithm Γ will eventually converge to the optimum. The question of the speed of convergence deserves more study. Now, we numerically compare how the proposed algorithm converges to the optimum with different ηs.

We run our distributed algorithm assuming that all nodes have the same power budget $\mathcal{P} = 7W$, and have the same utility weight $\omega_i = 1$. At iteration 0, the sensing rate is $s_i = 0$ at all nodes. We choose three different scale factors $\eta = \{0.5, 5, 10\}$ to run the algorithm, that minimizes the overall function A. Note that all three choices of η are much larger than the value given in Theorem 6.4. As shown in Figure 5, the algorithm converges to the optimum for all three step sizes. We see that the optimization reduces the objective function A from ∞ to 24.1. We also see that the convergence of the algorithm depends to a great extent on the value of η: a larger value of η may lead to faster convergence. From Figure 6.4 we see that for $\eta = 0.5, 5, 50$, the algorithm takes roughly 30000, 300 and 300 iterations to reduce A to within 10% of optimality.

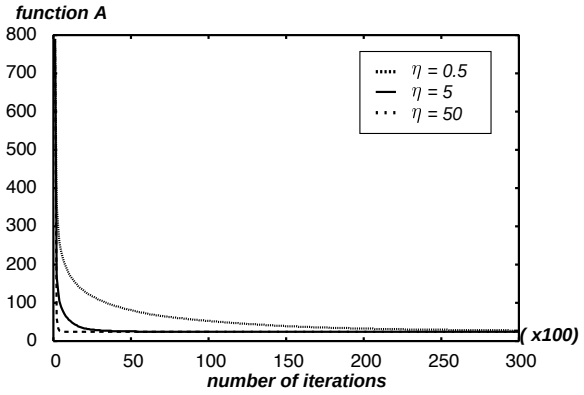

Fig. 5. Comparison of convergence speed for different ηs

2) Power budget affects optimization result: The energy collection rates of solar panels vary with weather condition, and thus affect power budget $\mathcal{P}$. We next demonstrate how power budgets change the network-wide power allocation and the aggregate sensing utility. We assume all nodes have the same power budget $\mathcal{P}$. We run our distributed algorithm for 7 different power budgets $\mathcal{P} = 7W \rightarrow 13W$, which correspond to 7 different weather conditions. Figure 6 shows the aggregated sensing utility increases as energy budget $\mathcal{P}$ increases. We also plot in the same figure the average sensing power on all nodes as $\mathcal{P}$ increases. The more power available is, the more data will be collected by sensors. Notice that both the utility curve and sensing power curve eventually flat out when $\mathcal{P}$ gets large. This is because when there is abundant power, all wireless links can operate at their maximum capacities, e.g. 11Mbps for $802.11b$ (goodput may vary). Consequently, the amount of data that can be sent to the sink is bounded from above. This upper bound is determined by both link maximum capacities and the network topology. Due to this data transmission limit, the aggregate sensing utility is also bounded, and there is no point for sensors to waste energy on collecting more data which can not be delivered to the sink.

Figure 7 shows the average power used for communication at all nodes for different energy budgets. As expected, as $\mathcal{P}$ increases from $7W$ to $9W$, sensors collect more and more data to be sent to the sink. Consequently, the overall communication power, both for transmitting and for receiving, increases. Interestingly, when $\mathcal{P}$ increases from $9W$ to $13W$, the communication power decreases slightly. To understand this somewhat counter-intuitive phenomenon, we looked into not only the aggregate data rate flowing into the sink, but also the sources of those data. When $\mathcal{P}$ is low, the major performance bottleneck is sensing, all sensed data can be completely delivered to the sink. Therefore, the larger $\mathcal{P}$, the more data collected by sensors, the higher the communication power. As seen in Figure 6, when $\mathcal{P} \geq 9W$, wireless links operate almost close to their full capacities. The aggregate data rate to the sink approaches its upper limit. Due to this data rate limit, not all sensors need to sense data at their full capacities. When $\mathcal{P}$ increases, sensors close to the sink have more power for sensing. Therefore in the optimal solution given by our algorithm, while the aggregate data rate is fixed, more and more data are from sensors close to the sink, consequently, we see a slightly decrease in communication power consumption.

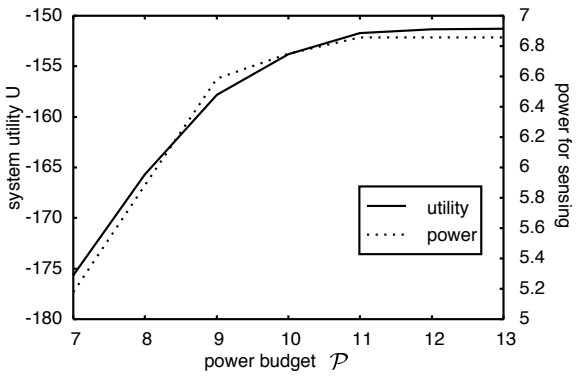

Fig. 6. Utility and sensing power increases as power budget increases

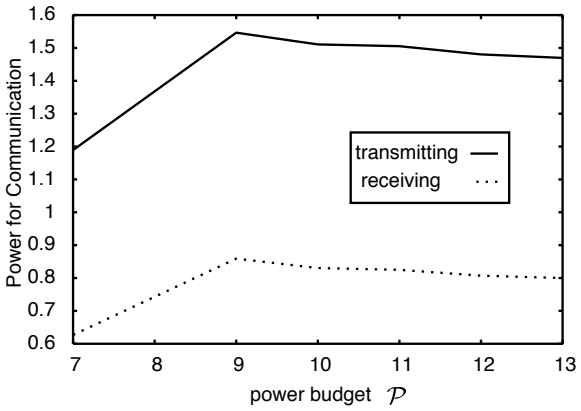

Fig. 7. Communication power changes as power budget increases

To further illustrate this, we compare in Figure 8(a), 8(b) and 8(c) the power allocation on a subset of node for $\mathcal{P} = 7, 9, 13W$. In Figure 8(a), when $\mathcal{P}$ is low, nodes far away from the sink, such as node $1, 7$ spend most of their power on sensing; nodes close to the sink, such as node $5, 6, 12, 17, 18$ are responsible for forwarding sensed data to the sink. On those nodes, the communication power is more than 33% of overall power budget. Consequently, the sensing power is lower than that of node 1 or 7. In Figure 8(b), when $\mathcal{P}$ increases to $9W$, all nodes have more power for sensing; nodes close to data sink, $6, 12, 18$, spend a large portion of power (50% or more) to forward data to the sink at their close-to-full goodput capacities, $1, 2, 5.5Mbps$ respectively. In Figure 8(c), when $\mathcal{P} = 13W$, because wireless links connecting to the sink are already saturated, the overall link data rates delivered to the sink only slight increases compared to 8(b). However, due to the concavity of the utility functions, nodes close to sink, such as $6, 12, 17, 18$ increase their sensing power further and generate more data, while nodes far way for the sink, such as node $1, 7$, have to reduce their sensing rates (and thus sensing power) accordingly. Now a larger portion of data are from sensors close to the sink, the power spent on data communication to the sink at $\mathcal{P} = 13W$ is lower than that at $\mathcal{P} = 9W$, as indicated in Figure 7. Actually, when $\mathcal{P} = 13W$, there is no longer power constraint at each and every node, the optimal sensing rates given by our distributed algorithm are thus max-min fair as proved in Theorem 7.1.

3) Adaptation to link failure and application needs: So far, we have demonstrated the performance of our algorithm using parameter settings with *static* network topology and *fixed* node utility weights (i.e., data collected at different nodes are equally important). In addition, we conducted simulations to evaluate how our algorithm adapts to link failures and changes of node utility weights. Next, we show two typical simulation results: one for link failure, and the other one for change of node utility weight. In both cases, we use power budget $\mathcal{P} = 7W$ and $\eta = 50$. Our algorithm would adapt and re-converge to 10% of optimality in $100 - 200$ iterations.

First, we show the performance of our algorithm in the case of link failure. In Figure 9(a), we plot the change of system utility when link $(11, 12)$ fails at iteration 5000 and then later comes back at iteration 10000. At iteration 5000, as link $(11, 12)$ fails, nodes with their sensed data forwarded over the failed link have to reduce their sensing rates. Consequently, the system utility decreases. As nodes start to find alternative paths to forward their sensed data

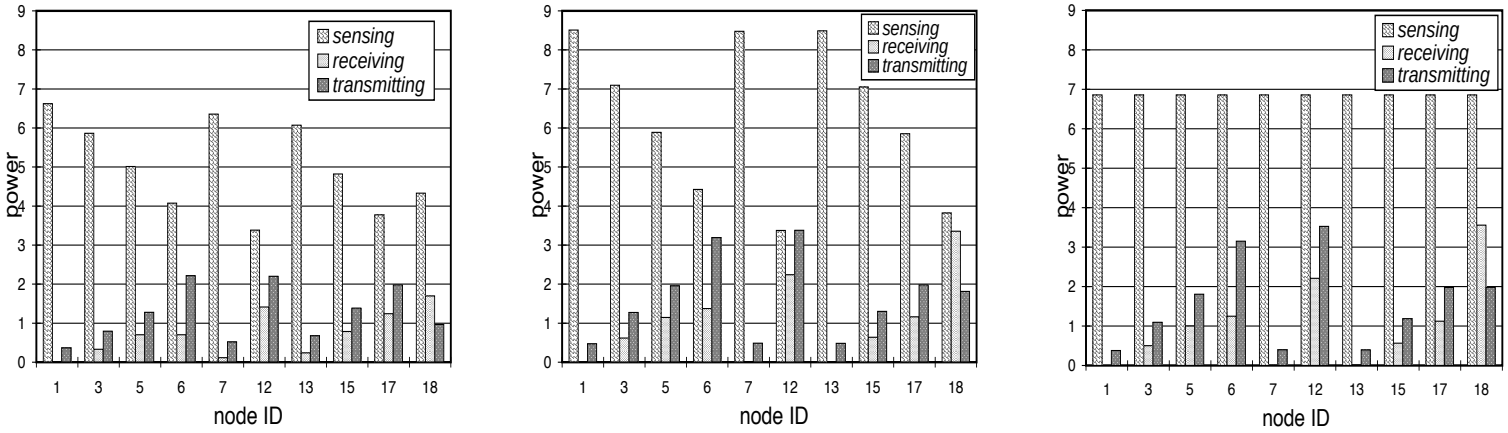

(a) Homogeneous when $\mathcal{P} = 7W$ (b) Homogeneous when $\mathcal{P} = 9W$ (c) Homogeneous when $\mathcal{P} = 13W$

Fig. 8. Individual node power consumption p_i for different power budgets and node utility weights

to data sinks, their sensing rates increase, and the system utility increases as well. At iteration 10000, when link $(11, 12)$ comes back, since nodes have already found alternative paths to forward their sensed data, the recovery of link $(11, 12)$ just slightly improve the system utility.

Second, we show the performance of our algorithm in the case of node utility weight change. In Figure 9(b), we plot the change of system utility when the weight of node 18 increases from 1 to 25 at iteration 5000 and later resets to be 1 at iteration 10000. At iteration 5000, node 18 increases its weight from 1 to 25. As expected, when node 18 starts to collect more data, nodes with data forwarded via node 18 would reduce their sensing data rates. The overall system utility decreases. At iteration 10000, node 18 reduces its weight from 25 to 1. When node 18 reduces its sensing rate, it starts to forward more data for other nodes. Therefore, other nodes will increase their data rates, and the system utility increases as well.

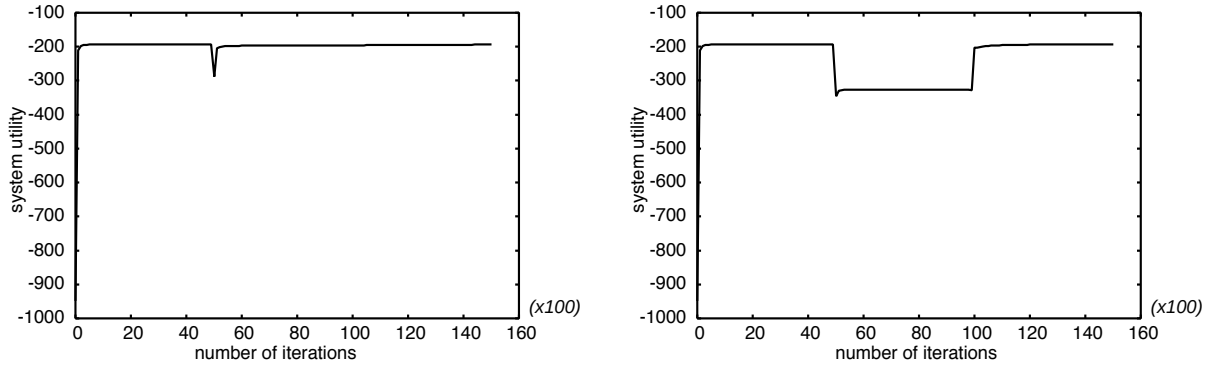

(a) Adaptation of our distributed algorithm to the failure and recovery of link $(11, 12)$

(b) Adaptation of our distributed algorithm to the change of utility weight at node 18

Fig. 9. Adaptation of our distributed algorithm to link failure and change of utility weight

VIII. Extensions and Variations

We have proposed a distributed algorithm for allocating energy between sensing and data routing in order to maximize the system utility in a network in which all data is routed to a common sink. In this section we discuss how this work can be extended to the case of multiple sink scenario, and to the case of more general resource constraints.

A. Extensions to the Multiple Sink Scenario

With multiple data sinks, we identify two problem formulations. In the first case, which we refer to as "single commodity routing": data can be routed to *any* one of multiple sinks. This model would be appropriate when the goal is to route data to a sensor network gateway that would make the data available to the outside world. In "multiple commodity routing", data injected at node i must be delivered to a predetermined node j. This model would be appropriate for data communication networks. Our distributed algorithm can be extended to solve the optimization problem under both single commodity routing and multiple commodity routing. In this paper, as our interest is wireless sensor networks, next, we discuss the single commodity case thoroughly, while the multiple commodity case briefly.

For single commodity routing, as shown in Figure 10, the multiple sink problem can be mapped to a single sink problem, in which all data traffic is destined to a virtual sink node via any of the multiple sinks. To implement this virtual node, our distributed algorithm needs to be modified slightly. Recall that for a single sink node $\odot$, the marginal cost for this sink node $\odot$, $\partial A^{\phi}(\phi)/\partial R_{\odot}$, is set to be 0. With multiple sink nodes $\{\odot_1, \ldots, \odot_m\}$, in order to implement this virtual sink node, we set $\partial A^{\phi}(\phi)/\partial R_{\odot_j} = 0$ for $j \in \{1, \ldots, m\}$. This is the only extension that is needed to take multiple sinks into account for single commodity routing.

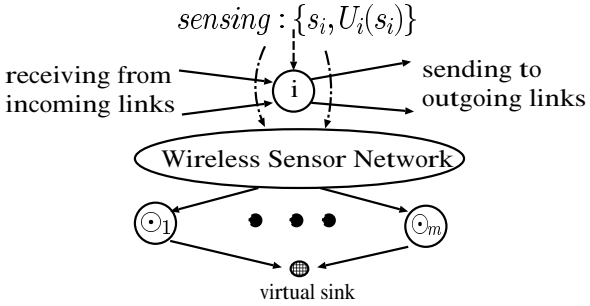

Fig. 10. Mapping from multiple sinks to single sinks

For multiple commodity routing, we have to introduce a dedicated set of routing variables $\phi(\odot_j)$ for each destination $\odot_j$. Consequently, for each destination $\odot_j$, we get a set of demand variables $R(\odot_j)$, a set of node traffic variables $t(\odot_j)$, a set of flow rate variables $f(\odot_j)$, and a set of blocking nodes $B(\odot_j)$. For each destination $\odot_j$, the distributed algorithm for updating the routing variable $\phi(\odot_j)$ is similar to that of a single destination: first, $\partial A^f(f)/\partial f_{kl}(\odot_j)$ is calculated using equation (26); second, $\partial A^{\phi}(\phi)/\partial \phi_{ik}(\odot_j)$ is calculated using equations (27) and (28); third, based on $\partial A^{\phi}(\phi)/\partial \phi_{ik}(\odot_j)$, we update $\phi(\odot_j)$ similar to that for a single destination. Following similar proofs, we are able to generalize Theorem 6.1, Theorem 6.2, Theorem 6.3, Theorem 6.4 to the case of multiple commodity routing, and prove the convergence of the generalized algorithm to the optimal solution. See [21] for more details. However, as indicated by [14] [12], in general, Theorem 7.1 does not hold for multiple commodity routing.

B. Extensions to exclusive transmission and reception model

For wireless networks with small node degree, we have used non-steerable directional antennas and non-overlapping channels to allow simultaneous data flow over all links. However, in the case of limited number of non-overlapping channels, and/or limited number of (but steerable) directional antennas, simultaneous data flow over all links may not be possible. Next, we extend our algorithm to exclusive transmission and reception model as introduced in [22]: a node can only transmit or receive packets at any time.

For exclusive transmission and reception model, [22] proved the NP-hardness of the problem, and provided a heuristic solution. The heuristic solution requires that the node utilization (overall time fraction in data transmission and reception over all incoming and outgoing links) must be bounded by $2/3$.

$$\sum_{(i,k)\in L_O(i)} \tau_{ik} + \sum_{(k,i)\in L_I(i)} \tau_{ki} \leq 2/3 \tag{42}$$

Next, based on equation (42), we extend our distributed algorithm to achieve $1/3$ of maximum utility.

At each node i, we introduce additional convex and increasing penalty function $g_i(\tau_{ik} \in L_O(i), \tau_{ki} \in L_I(i))$ to replace the time fraction constraint given by equation (42). We have,

$$\lim_{\sum_{(i,k)\in L_O(i)} \tau_{ik} + \sum_{(k,i)\in L_I(i)} \tau_{ki} \to 2/3} g_i(\tau_{ik} \in L_O(i), \tau_{ki} \in L_I(i)) \to \infty \tag{43}$$

The optimization goal is thus $A = Y + D + Z + G$, where $G = \sum_i g_i(\tau_{ik} \in L_O(i), \tau_{ki} \in L_I(i))$.

As shown by [22], if the time fraction constraints given by equation (42) are satisfied, the scheduling problem can be further solved optimally using centralized algorithms (*maximum weighted matching*) or 2-approximate distributed algorithms (*greedy matching*).

Using *greedy matching* to solve the scheduling problem, our fully-distributed algorithm would guarantee to achieve $1/3$ of optimality. First, the optimal sensing rates s^* must satisfy the sufficient condition as follows.

$$\sum_{(i,k)\in L_O(i)} \tau_{ik} + \sum_{(k,i)\in L_I(i)} \tau_{ki} \leq 1 \tag{44}$$

Therefore, $\frac{2s^*}{3}$, which satisfies the time fraction constraints, would achieve $\frac{2U(s^*)}{3}$ because of the concavity of utility functions. The system utility is further reduced by $1/2$ due to the approximation ratio of the greedy matching algorithm. Overall, our fully-distributed algorithm would guarantee to achieve $1/3$ of optimality.

IX. Conclusion

In this paper, we proposed an optimal sensing and routing strategy for energy constrained wireless sensor networks with non-steerable directional antennas. We first formulated a joint sensing rate control, data routing and energy allocation problem. We then converted the combined sensing/routing problem into a unified routing problem. A distributed algorithm was developed for all nodes to co-operatively drive the sensor network to its optimal operation point, where the network-wide sensing utility is maximized under node power constraints. Simulations for a network of small solar powered X-band radars illustrated the operation of our distributed algorithm. The trade-off between sensing and communication was illustrated in different simulation settings on power collection rates.

Further research can be pursued in the following directions:

- Our simulation results are encouraging. We plan to implement our distributed algorithm in a network of X-band radars currently under development. We are especially interested in testing how our algorithm adapts to real environmental conditions, such as the strength of sunshine, the link goodput probabilities, and the location and movement of sensed objects.
- In this paper we have not considered a sensor node's consumption of power for computation. This factor will become more important as processing demands increase, e.g., if compression is performed before data transmission. Then there is a trade-off on power allocation between processing and routing. In the case of compression, the more one node compress, the less data the network will have to transmit to the sink. We plan to incorporate computation into our framework in future work.
- In our current formulation, we assume sensing utility is elastic and try to maximize the aggregate utility as long as the power consumption on each node is lower than its power expenditure budget. A dual formulation is to minimize aggregate power consumption given that the aggregate/individual sensing utilities are above some threshold. This may be a more appropriate problem formulation to consider if one want to maximize the life time of a sensor network under a given energy constraint.

Acknowledgment

This research was supported in part by the National Science Foundation under NSF grants ANI-9980552, ANI-0085848, and the Engineering Research Centers Program, award number EEC-0313747 001. Any opinions, findings, and conclusions or recommendations expressed in this material are those of the authors and do not necessarily reflect the views of the funding agencies.

REFERENCES

[1] D. Estrin, D. Culler, and K. Pister, "Connecting the physical world with pervasive networks," in *IEEE Pervasive Computing*, 2002.

[2] B. Donovan, D. J. McLaughlin, J. Kurose, and V. Chandrasekar, "Principles and design considerations for short-range energy balanced radar networks," in *Proceedings of IEEE Geoscience and Remote Sensing Society*, 2005.

[3] A. Kansal, D. Potter, and M. B. Srivastava, "Performance aware tasking for environmentally powered sensor networks," in *Proceedings of ACM SIGMETRICS*, 2004.

[4] R. Gallager and S. J. Golestaani, "Flow control and routing algorithms for data networks," in *ICCC*, Atlanta, 1980, pp. 779–784.

[5] L. Xiao, M. Johansson, and S. Boyd, "Simultaneous routing and resource allocation via dual decomposition," *IEEE Transactions on Communications*, vol. 52, no. 7, pp. 1136–1144, 2004.

[6] X. Lin and N. B. Shroff, "Joint rate control and scheduling in multihop wireless networks," in *43rd IEEE Conference on Decision and Control*, 2004.

[7] L. Chen, S. H. Low, M. Chiang, and J. C. Doyle, "Optimal cross-layer congestion control, routing and scheduling design in ad hoc wireless networks," in *Proceedings of IEEE INFOCOM*, 2006.

[8] R. G. Gallager, "A minimum delay routing algorithm using distributed computation," in *IEEE Transaction on Communications*, january 1977, pp. 73–85.

[9] F. Kelly, A. Maulloo, and D. Tan, "Rate control in communication networks: shadow prices proportional fairness and stability," *Journal of the Operational Research Society*, 1998.

[10] F. Kelly, "Charging and rate control for elastic traffic," *European Transaction on Telecommunications*, vol. 8, pp. 33–37, 1997.

[11] Y. Xue, Y. Cui, and K. Nahrstedt, "A utility-based distributed maximum lifetime routing algorithm forwireless networks," in *Second International Conference on Quality of Service in Heterogeneous Wired/Wireless Networks*, 2005.

[12] X. Lin and N. B. Shroff, "The impact of imperfect scheduling on cross-layer rate control in multihop wireless networks," in *Proceedings of IEEE INFOCOM*, 2005.

[13] L. Bui, A. Eryilmaz, R. Srikant, and X. Wu, "Joint asynchronous congestion control and distributed scheduling for multihop wireless networks," in *Proceedings of IEEE INFOCOM*, 2006.

[14] A. Eryilmaz and R. Srikant, "Fair resource allocation in wireless networks using queue-length-based scheduling and congestion control," in *Proceedings of IEEE INFOCOM*, 2005.

[15] A. Mishra, V. Shrivastava, S. Banerjee, and W. Arbaugh, "Partially-overlapped channels not considered harmful," in *ACM Sigmetrics*, 2006.

[16] J. Robinson, K. Papagiannaki, C. Diot, X. Guo, and L. Krishnamurthy, "Experimenting with a multi-radio mesh networking testbed," in *1st workshop on Wireless Network Measurements*, 2005.

[17] S. Boyd, *Convex Optimization*. Cambridge University Press, 2004.

[18] B. Radunovic and J. L. Boudec, "A unified framework for max-min and min-max fairness with applications," in *Proceedings of 40th Annual Allerton Conference on Communication, Control, and Computing*, 2002.

[19] D. Nace, L. N. Doan, E. Gourdin, and B. Liau, "Optimal max-min fair resource allocation for elastic flows," *To appear in IEEE Transactions on Networking*, December 2006.

[20] B. Donovan and D. J. McLaughlin, "Improved radar sensitivity through limited sector scanning: The dcas approach," in *Proceedings of AMS Radar Meteorology*, 2005.

[21] C. Zhang, J. Kurose, Y. Liu, and D. Towsley, "An optimal distributed algorithm for joint resource allocation and routing in node-based wireless networks," in *UMass CMPSCI Technical Report 05-43*, 2005.

[22] M. Kodialam and T. Nandagopal, "Characterizing achievable rates in multi-hop wireless networks: The joint routing and scheduling problem," in *MobiCom*, 2003.

[23] D. G. Luenberger, *Linear and Nonlinear Programming*. Kluwer Academic Publishers, 2003.

X. APPENDIX A

Next is the proof for Theorem 5.1. It was proved in [8]. We include it for completeness.

Proof:

Summing both sides of equation (24) over i, we see that any solution to (24) satisfies

$$t_{\odot} = \sum_i R_i. \tag{A1}$$

Temporarily let $\phi_{\odot i} = R_i/t_{\odot}$ and substitute this in (24).

$$t_i = \sum_{l=1}^{|\mathcal{V}|} t_l \phi_{li}. \tag{A2}$$

Any solution to (A1) and (A2) satisfies (24) and vice versa. Let $\hat{\Phi}$ be the $|\mathcal{V}| \times |\mathcal{V}|$ matrix with components ϕ_{li}. $\hat{\Phi}$ is stochastic (i.e., $\phi_{li} \geq 0$ for all l, i and $\sum_i \phi_{li} = 1$ for all l) and (A2) is just the formula for steady-state probabilities in a Markov chain.

It is well know that if $\hat{\Phi}$ is irreducible, then (A2) has a unique solution, aside from a scale factor determined by (A1), and $t_i > 0$, $1 \leq i \leq |\mathcal{V}|$. The matrix $\hat{\Phi}$ is irreducible; however, if for each i, k there is a path $i, l, m, \ldots, p, k$

such that $\phi_{il} > 0$, $\phi_{lm} > 0$, ..., $\phi_{pk} > 0$. If $R_i > 0$ for $1 \leq i \leq |\mathcal{V}| - 1$, then node $\odot$ has a path to each i, $1 \leq i \leq |\mathcal{V}| - 1$. By the definition of routing variables, each i has a path to $\odot$ and consequently $\hat{\Phi}$ is irreducible. Thus (24) has a unique solution, with positive t_i, if $R_i > 0$ for $1 \leq i \leq |\mathcal{V}| - 1$.

Now let $t = (t_1, \ldots, t_{|\mathcal{V}|-1})$, $R = (R_1, \ldots, R_{|\mathcal{V}|-1})$ and let Φ be the $|\mathcal{V}| - 1 \times |\mathcal{V}| - 1$ matrix with components $\phi_{li} (1 \leq i, l \leq |\mathcal{V}| - 1)$. Equation (24) for $1 \leq i \leq |\mathcal{V}| - 1$ is then $t(I - \Phi) = R$. Since this equation has a unique solution for $R_i > 0$, $I - \Phi$ must have an inverse, and

$$t = R(I - \Phi)^{-1} \tag{A3}$$

Since the components of t are positive when the components of R are positive, components of t are nonnegative when the components of R are nonnegative. Differentiating (A3), we get the continuous function of Φ

$$\frac{\partial t_i}{\partial R_l} = [(I - \Phi)^{-1}]_{li} \tag{A4}$$

Using (A4) in (A3), the solution to (24) is conveniently expressed, for any t, as

$$t_i = \sum_l \frac{\partial t_i}{\partial R_l} R_l \tag{A5}$$

Finally, differentiating (24) with respect to ϕ_{km}, we get

$$\frac{\partial t_i}{\partial \phi_{km}} = \sum_{l=1}^{|\mathcal{V}|-1} \frac{\partial t_l}{\partial \phi_{km}} \phi_{li} + t_k \delta_{im}$$

where $\delta_{im} = 1$ for $i = m$ and 0 and otherwise. For fixed k, m, this is the same of equations as (24), so that the solution, continuous in ϕ, is

$$\frac{\partial t_i}{\partial \phi_{km}} = \frac{\partial t_i}{\partial R_m} t_k \tag{A6}$$

■

XI. Appendix B

Next is the proof for Theorem 6.1.

Proof:

First we show that (27), repeated below, has a unique solution.

$$\frac{\partial A^\phi(\phi)}{\partial R_i} = \sum_k \phi_{ik} \left[\frac{\partial A^f(f)}{\partial f_{ik}} + \frac{\partial A^\phi(\phi)}{\partial R_k} \right] \tag{B1}$$

Let $b_i = \sum_k \phi_{ik} \partial A^f(f) / \partial f_{ik}$ and let b the column vector $(b_1, \ldots, b_n)$. Let $\nabla \bullet A^\phi$ be the column vector $(\partial A^\phi(\phi)/\partial R_1, \ldots, \partial A^\phi(\phi)/\partial R_n)$ Then (B1) can be rewritten as

$$\nabla \bullet A^\phi = b + \Phi(\nabla \bullet A^\phi). \tag{B2}$$

We saw in the proof of Theorem 5.1 that $I - \Phi$ has a unique inverse with components given by (A4). Thus the unique solution to (B2) is

$$\frac{\partial A^\phi(\phi)}{\partial R_i} = \sum_l \frac{\partial t_l}{\partial R_i} \sum_m \phi_{lm} \frac{\partial A^f(f)}{\partial f_{lm}} \tag{B3}$$

$$= \sum_{l,m} \frac{\partial f_{lm}}{\partial R_i} \frac{\partial A^f(f)}{\partial f_{lm}} \tag{B4}$$

Differentiating $\partial A^\phi(\phi)$ directly with (25), we get the same unique solution, which, from Theorem 5.1, is continuous in ϕ.

Finally we calculate $\partial A^\phi(\phi)/\partial\phi_{ik}$ directly using (25),

$$\begin{aligned}\frac{\partial A^\phi(\phi)}{\partial\phi_{ik}} &= \sum_{l,m}\frac{\partial A^f(f)}{\partial f_{lm}}\phi_{lm}\frac{\partial t_l}{\partial\phi_{ik}}+\frac{\partial A^f(f)}{\partial f_{ik}}t_i \\ &= t_i\left[\sum_{l,m}\frac{\partial A^f(f)}{\partial f_{lm}}\phi_{lm}\frac{\partial t_l}{\partial R_k}\right]+t_i\frac{\partial A^f(f)}{\partial f_{ik}} \\ &= t_i\left[\frac{\partial A^\phi(\phi)}{\partial R_k}+\frac{\partial A^f(f)}{\partial f_{ik}}\right] \end{aligned} \tag{B5}$$

■

We have used (A6) and (B3) to derive (B5), which is the same as (28). This is clearly continuous in ϕ given the continuity of t_i and $\partial A^\phi(\phi)/\partial R_i$, and the proof is complete.

XII. Appendix C

Next is the proof for Theorem 6.2.

Proof:

First we show that (29) is a necessary condition to minimize A^ϕ by assuming that ϕ does not satisfy (29). This means that there is some i,k and m such that

$$\phi_{ik}>0,\quad \frac{\partial A^\phi(\phi)}{\partial\phi_{ik}}>\frac{\partial A^\phi(\phi)}{\partial\phi_{im}} \tag{C1}$$

Since these derivatives are continuous, a sufficiently small increase in ϕ_{im} and corresponding decrease in ϕ_{ik} will decrease A^ϕ, thus establishing that ϕ does not minimize A^ϕ.

Next we show that (30), repeated below, is a sufficient condition to minimize A^ϕ.

$$\frac{\partial A^f(f)}{\partial f_{ik}}+\frac{\partial A^\phi(\phi)}{\partial R_k}\ \geq\ \frac{\partial A^\phi(\phi)}{\partial R_i},\quad \text{all } i,k. \tag{C2}$$

Suppose that ϕ satisfies (C2) and has link data rates f and node data rates t. Let ϕ^* be any other set of routing variables with link data rates f^* and node data rates t^*. Define

$$f(\lambda)=(1-\lambda)f+\lambda f^* \tag{C3}$$

$$A^f(\lambda)=A^f(f(\lambda)) \tag{C4}$$

Since A^f is a convex, non-decreasing function of the flow rate sets f, therefore $A^f(\lambda)$, is convex in λ, and hence

$$\left.\frac{dA^f(\lambda)}{d\lambda}\right|_{\lambda=0}\leq A^\phi(\phi^*)-A^\phi(\phi) \tag{C5}$$

Since ϕ^* is arbitrary, proving that $dA^f(\lambda)/d\lambda\geq 0$ at $\lambda=0$ will complete the proof. From (C3) and (C4),

$$\left.\frac{dA^f(\lambda)}{d\lambda}\right|_{\lambda=0}=\sum_{i,k}\frac{\partial A^f(f)}{\partial f_{ik}}\left(f^*_{ik}-f_{ik}\right) \tag{C6}$$

We now show that

$$\sum_{i,k}\frac{\partial A^f(f)}{\partial f_{ik}}f^*_{ik}\geq\sum_k R_k\frac{\partial A^\phi(\phi)}{\partial R_k} \tag{C7}$$

Note from (C2) that

$$\sum_k\frac{\partial A^f(f)}{\partial f_{ik}}\phi^*_{ik}\geq\frac{\partial A^\phi(\phi)}{\partial R_i}-\sum_k\frac{\partial A^\phi(\phi)}{\partial R_k}\phi^*_{ik} \tag{C8}$$

Multiplying both sides of (C8) by t_i^*, summing over i, and recalling that $f_{ik}^* = t_i^* \phi_{ik}^*$ (see (25)) , we obtain

$$\sum_{i,k} \frac{\partial A^f(f)}{\partial f_{ik}} f_{ik}^* \geq \sum_i t_i^* \frac{\partial A^\phi(\phi)}{\partial R_i} - \sum_{i,k} t_i^* \phi_{ik}^* \frac{\partial A^\phi(\phi)}{\partial R_k} \tag{C9}$$

From (24), $\sum_i t_i^* \phi_{ik}^* = t_k^* - R_k$. Substituting this into the rightmost term of (C9) and canceling, we get (C7). Note that the only inequality used here was (C8), and that if ϕ is substituted for ϕ^*, this becomes an equality from the equation for $\frac{\partial A^\phi(\phi)}{\partial R_i}$ in (27). Thus

$$\sum_{i,k} \frac{\partial A^f(f)}{\partial f_{ik}} f_{ik} = \sum_k R_k \frac{\partial A^\phi(\phi)}{\partial R_k} \tag{C10}$$

Substituting (C7) and (C10) into (C6), we see that $dA^f(\lambda)/d\lambda \geq 0$ at $\lambda = 0$, completing the proof.

■

XIII. Appendix D

We prove Theorem 6.4 through a sequence of seven lemmas. The first five establish the descent properties of the algorithm, the sixth establishes a type of continuity condition, showing that if ϕ does not minimize A^ϕ, the for any ϕ^* in a neighborhood of ϕ, $A^\phi(\Gamma^m(\phi^*)) < A^\phi(\phi)$ for some m. The seventh lemma is a global convergence theorem which does not require continuity in the algorithm Γ; Lemmas 13.6 and 13.7 together establish Theorem 6.4.

Let ϕ be an arbitrary set of routing variables satisfying $A^\phi(\phi) < A_0$ for some A_0. Let $\phi^1 = \Gamma(\phi)$ and let t, f, t^1, f^1 be the node and link data rates corresponding to ϕ and ϕ^1, respectively. Let f^λ, $(0 \leq \lambda \leq 1)$ be defined by $f_{ik}^\lambda = (1-\lambda) f_{ik} + \lambda f_{ik}^1$, and let

$$A^f(\lambda) = A^f(f(\lambda)) \tag{D1}$$

From the Taylor remainder theorem,

$$A^\phi(\phi^1) - A^\phi(\phi) = \left.\frac{dA^f(\lambda)}{d\lambda}\right|_{\lambda=0} + \frac{1}{2} \left.\frac{d^2 A^f(\lambda)}{d\lambda^2}\right|_{\lambda=\lambda^*} \tag{D2}$$

where λ^* is some number, $0 \leq \lambda^* \leq 1$. The continuity of the second derivative above will be obvious from the proof of Lemma 13.4, which upper bounds that term. The first three lemmas deal with $\frac{dA^f(\lambda)}{d\lambda}|_{\lambda=0}$.

Lemma 13.1:

$$\left.\frac{dA^f(\lambda)}{d\lambda}\right|_{\lambda=0} = \sum_{i,k} -\Delta_{ik} a_{ik} t_i^1 \tag{D3}$$

Proof: Using the definitions of a_{ik} and Δ_{ik} in (32) and (33),

$$\begin{aligned}
\sum_k \Delta_{ik} a_{ik} &= \sum_{k \neq k_{min}(i)} [\phi_{ik} - \phi_{ik}^1] \left\{ \frac{\partial A^f(f)}{\partial f_{ik}} + \frac{\partial A^\phi(\phi)}{\partial R_k} - \min_{m \notin B_i} \left[\frac{\partial A^f(f)}{\partial f_{im}} + \frac{\partial A^\phi(\phi)}{\partial R_m} \right] \right\} \\
&= \sum_k [\phi_{ik} - \phi_{ik}^1] \left[\frac{\partial A^f(f)}{\partial f_{ik}} + \frac{\partial A^\phi(\phi)}{\partial R_k} \right] \qquad \text{(D4)} \\
&= \frac{\partial A^\phi(\phi)}{\partial R_i} - \sum_k \phi_{ik}^1 \left[\frac{\partial A^f(f)}{\partial f_{ik}} + \frac{\partial A^\phi(\phi)}{\partial R_k} \right] \qquad \text{(D5)}
\end{aligned}$$

In (D4), we have used (34) to extend the sum over all k and in (D5), we have used (27). Multiplying both sides of (D5) by t_i^1, summing, and using (24) and (25), we get

$$\begin{aligned}
\sum_{i,k} \Delta_{ik} a_{ik} t_i^1 &= \sum_i t_i^1 \frac{\partial A^\phi(\phi)}{\partial R_i} - \sum_{i,k} f_{ik}^1 \frac{\partial A^f(f)}{\partial f_{ik}} - \sum_k \left[t_k^1 - R_k \right] \frac{\partial A^\phi(\phi)}{\partial R_k} \\
&= -\sum_{i,k} f_{ik}^1 \frac{\partial A^f(f)}{\partial f_{ik}} + \sum_k R_k \frac{\partial A^\phi(\phi)}{\partial R_k} \qquad \text{(D6)} \\
&= \sum_{i,k} (f_{ik} - f_{ik}^1) \frac{\partial A^f(f)}{\partial f_{ik}} \qquad \text{(D7)} \\
&= -\left.\frac{dA^f(\lambda)}{d\lambda}\right|_{\lambda=0} \qquad \text{(D8)}
\end{aligned}$$

We have used (C10) to get (D7), and (D8) from (D1), completing the proof. ■

Lemma 13.2:

$$\left.\frac{dA^f(\lambda)}{d\lambda}\right|_{\lambda=0} \leq -\frac{1}{\eta(|\mathcal{V}|-1)^3}\sum_i \Delta_i^2 t_i^2 \tag{D9}$$

where

$$\Delta_i = \sum_k \Delta_{ik} \tag{D10}$$

Proof: From the definition of Δ_{ik} in (33), $-a_{ik} \leq -t_i\Delta_{ik}/\eta$. Substituting this into (D3) yields

$$\begin{aligned}\left.\frac{dA^f(\lambda)}{d\lambda}\right|_{\lambda=0} &\leq -\frac{1}{\eta}\sum_{i,k}\Delta_{ik}^2 t_i t_i^1 \\ &\leq -\frac{1}{(|\mathcal{V}|-1)\eta}\sum_i \Delta_i^2 t_i t_i^1 \end{aligned}\tag{D11}$$

where (D11) follows from Cauchy's inequality, $(\sum_k \alpha_k\beta_k)^2 \leq (\sum \alpha_k^2)(\sum \beta_k^2)$, with $\alpha_k = 1$, $\beta_k = \Delta_{ik}$, and the sum over $k \neq i$.

Now define t_i^* as the total flow at node i if the routing variables ϕ_{ik} (for $k \neq k_{min}(i)$) are reduced by Δ_{ik} but ϕ_{ik} for $k = k_{min}(i)$ is not increased. Mathematically t_i^* satisfies

$$t_i^* = \sum_l t_l^*[\phi_{li} - \Delta_{li}] + R_i \tag{D12}$$

This has a unique solution because of the loop freedom of ϕ. Subtracting (D12) from (24) results in

$$t_i - t_i^* = \sum_l [t_l - t_l^*]\phi_{li} + \sum_l t_l^*\Delta_{li} \tag{D13}$$

From (A5), using $\sum_l t_l^*\Delta_{li}$ for r_i,

$$t_i - t_i^* = \sum_l \frac{\partial t_i}{\partial R_l}\sum_k t_k^*\Delta_{kl} \tag{D14}$$

Since ϕ is loop-free, $\partial t_i/\partial R_l \leq 1$. Also if $\partial t_i/\partial R_l > 0$, then l is upstream of i and ϕ_{il} (and hence Δ_{il}) is zero. Thus

$$t_i - t_i^* \leq \sum_l \sum_{k\neq i} t_k^*\Delta_{kl} = \sum_{k\neq i} t_k^*\Delta_k \tag{D15}$$

Multiplying the left side by $\Delta_i \leq 1$ preserves the inequality, yielding

$$t_i\Delta_i \leq \sum_k t_k^*\Delta_k \tag{D16}$$

Since the right-hand side of (D14) is nonnegative, we also have $t_i\Delta_i \geq t_i^*\Delta_i$. We interrupt the proof now for a short technical lemma, which was proved by [8]. We include it here for completeness. The lemma will be used for further proof.

Lemma 13.3: Let α_i, $\beta_i (1 \leq i \leq m)$ be nonnegative numbers satisfying $\alpha_i \leq \sum_k \beta_k$; $\alpha_i \geq \beta_i$ for $1 \leq i \leq m$. Then

$$\sum_{i=1}^m \alpha_i\beta_i \geq \frac{1}{m^2}\sum_i \alpha_i^2 \tag{D17}$$

Proof:

$$\sum_i \alpha_i\beta_i \geq \sum_i \beta_i^2 \geq \frac{1}{m}(\sum \beta_i)^2 \tag{D18}$$

where we have used $\alpha_i \geq \beta_i$ and then Cauchy's inequality. Since $\sum \beta_i \geq \alpha_k$ for all k,

$$\sum_i \alpha_i\beta_i \geq \frac{1}{m}\alpha_k^2, \quad \text{for all } k. \tag{D19}$$

This implies (D17), completing the proof of Lemma (13.3). ■

Now let $\alpha_i = t_i\Delta_i$ and $\beta_i = t_i^*\Delta_i$. Since these terms are nonzero only for $i \neq \odot$, we can take $m = |\mathcal{V}| - 1$. Since the conditions of the lemma are satisfied for this choice,

$$\sum_i \Delta_i^2 t_i t_i^* \geq \frac{1}{(|\mathcal{V}|-1)^2} \sum_i \Delta_i^2 t_i^2. \tag{D20}$$

Since $t_i^* \leq t_i^1$, we can substitute (D20) into (D11), getting (D9) and completing the proof of Lemma (13.2).

Lemma 13.4: Let M be an upper bound of $\frac{\partial^2 A^f(f^\lambda)}{\partial f^\lambda_{l_1 m_1} \partial f^\lambda_{l_2 m_2}}$ over all l_1, m_1, l_2, m_2 and over $0 \leq \lambda \leq 1$. Then for any λ, $0 \leq \lambda \leq 1$,

$$\frac{d^2 A^f(\lambda)}{d\lambda^2} \leq M(|\mathcal{V}|+2)|\mathcal{V}|^2(|\mathcal{V}|-1)\sum_{j,k} \Delta_k^2 t_k^2 \tag{D21}$$

Proof: The bound M must exist because $\frac{\partial A^f(\lambda)}{\partial f^\lambda_{l_1 m_1} \partial f^\lambda_{l_2 m_2}}$ is a continuous function of λ over the compact region $0 \leq \lambda \leq 1$. Taking the second derivative, we get

$$\begin{aligned}
\frac{d^2 A^f(\lambda)}{d\lambda^2} &= \sum_{l_1,m_1} \sum_{l_2,m_2} \frac{\partial^2 A^f(\lambda)}{\partial f^\lambda_{l_1 m_1} \partial f^\lambda_{l_2 m_2}} (f^1_{l_1 m_1} - f_{l_1 m_1})(f^1_{l_2 m_2} - f_{l_2, m_2}) \\
&\leq \sum_{l_1 m 1} \sum_{l_2 m_2} M |f^1_{l_1 m_1} - f_{l_1 m_1}||f^1_{l_2 m_2} - f_{l_2 m_2}| \\
&\leq \sum_{i,k} M|L||f^1_{ik} - f_{ik}|^2 \\
&\leq \sum_{i,k} M|\mathcal{V}|(|\mathcal{V}|-1)|f^1_{ik} - f_{ik}|^2
\end{aligned} \tag{D22}$$

We now upper bound $|f^1_{ik} - f_{ik}|$ by first upper bounding $|t^1_i - t_i|$. As in the proof of Lemma 13.2, we have

$$\begin{aligned}
t^1_i - t_i &= \sum_l [t^1_l - t_l]\phi^1_{li} + \sum_l t_l[\phi^1_{li} - \phi_{li}] \\
&= \sum_l \frac{\partial t^1_i}{\partial R_l} \sum_k t_k[\phi^1_{kl} - \phi_{kl}]
\end{aligned} \tag{D23}$$

Since $0 \leq \partial t^1_i / \partial R_l \leq 1$, we can upper bound this by

$$t^1_i - t_i \leq \sum_k t_k \Delta_k$$

We can lower bound (D23) in the same way, considering only terms in which $\phi^1_{kl} - \phi_{kl} < 0$, and this leads to

$$|t^1_i - t_i| \leq \sum_k t_k \Delta_k \tag{D24}$$

$$f^1_{ik} - f_{ik} = [t^1_i - t_i]\phi^1_{ik} + t_i[\phi^1_{ik} - \phi_{ik}]$$

$$|f^1_{ik} - f_{ik}| \leq \sum_l t_l \Delta_l \phi^1_{ik} + t_i|\phi^1_{ik} - \phi_{ik}| \tag{D25}$$

The sum in (D25) has at most $|\mathcal{V}| - 1$ nonzero terms ($i \neq \odot$). Using Cauchy's inequality on both terms together, we get

$$|f^1_{ik} - f_{ik}|^2 \leq |\mathcal{V}| \left\{ \sum_l t_l^2 \Delta_l^2 [\phi^1_{ik}]^2 + t_i^2 [\phi^1_{ik} - \phi_{ik}]^2 \right\}$$

$$\sum_k |f^1_{ik} - f_{ik}|^2 \leq |\mathcal{V}| \left\{ \sum_l t_l^2 \Delta_l^2 + 2 t_i^2 \Delta_i^2 \right\} \tag{D26}$$

Summing over i and substituting the result in (D22),we get (D21) completing the proof. ■

Lemma 13.5: For given A_0, define

$$M = \max_{l_1,m_1,l_2,m_2} \max_{f:A^f(f)\le A_0} \frac{\partial^2 A^f(f)}{\partial f_{l_1 m_1} \partial f_{l_2 m_2}}(f) \tag{D27}$$

$$\eta = [M|\mathcal{V}|^7]^{-1}. \tag{D28}$$

Then for all ϕ such that $A^\phi(\phi) \le A_0$,

$$A^\phi(\phi^1) - A^\phi(\phi) \le -\frac{1}{2\eta(|\mathcal{V}|-1)^3} \sum_i \Delta_i^2 t_i^2. \tag{D29}$$

Proof: Temporarily let M be as defined in Lemma 13.4. Combining Lemma 13.2 and Lemma 13.4,

$$A^\phi(\phi^1) - A^\phi(\phi) \le \left[-\frac{1}{\eta(|\mathcal{V}|-1)^3} + \frac{M(|\mathcal{V}|+2)|\mathcal{V}|^2(|\mathcal{V}|-1)}{2} \right] \sum_i \Delta_i^2 t_i^2. \tag{D30}$$

For $\eta = [M|\mathcal{V}|^7]^{-1}$, the second term in brackets above is less than half the magnitude of the first term, yielding (D29). It follows that $A^\phi(\phi^1) \le A^\phi(\phi) \le A_0$. By convexity then $A^f(f^\lambda) \le A_0$ for $0 \le \lambda \le 1$. Thus M as given in (D27) satisfies the condition on M in Lemma 13.4, completing the proof. ■

Lemma 13.6: Let the scale factor η satisfy (D28) for a given A_0 and let ϕ be an arbitrary set of routing variables that does not minimize A^ϕ and satisfies $A^\phi(\phi) \le A_0$. Given this ϕ, there exists and $\epsilon > 0$ and an m, $1 \le m \le n$, such that for all ϕ^* satisfying $|\phi - \phi^*| < \epsilon$,

$$A^\phi(\Gamma^m(\phi^*)) < A^\phi(\phi) \tag{D31}$$

Proof: We consider three cases. The first is the typical case in which no blocking occurs and $A^\phi(\Gamma(\phi)) < A^\phi(\phi)$, the second is the case in which blocking occurs, and the third is the case in which $A^\phi(\Gamma(\phi)) = A^\phi(\phi)$.

Case 1: No blocking; $\Delta_i t_i > 0$ for some i. If no nodes are blocked for ϕ, then by the definition of blocking (36), there is a neighborhood of ϕ^* around ϕ for which no blocking occurs. In this neighborhood,

$$a_{ik} = \left[\frac{\partial A^f(f)}{\partial f_{ik}} + \frac{\partial A^\phi(\phi)}{\partial R_k} \right] - \min_{1\le m\le|\mathcal{V}|} \left[\frac{\partial A^f(f)}{\partial f_{im}} + \frac{\partial A^\phi(\phi)}{\partial R_m} \right] \tag{D32}$$

which is continuous in ϕ. It follows from (33) that Δ_{ik} is continuous in ϕ, and the upper bound to $A^\phi(\Gamma(\phi)) - A^\phi(\phi)$ in (D29) is continuous in ϕ. Since by assumption the bound in (D29) is strictly negative, there is a neighborhood of ϕ^* around ϕ for which

$$A^\phi(\Gamma(\phi^*)) - A^\phi(\phi^*) < -\frac{1}{4\eta(|\mathcal{V}|-1)^3} \sum_i \Delta_i^2 t_i^2 \tag{D33}$$

where Δ_i and t_i correspond to the given ϕ. Choose ϵ small enough so that (D33) is satisfied for $|\phi - \phi^*| < \epsilon$ and also so that

$$|A^\phi(\phi^*) - A^\phi(\phi)| \quad < \quad \frac{1}{4\eta(|\mathcal{V}|-1)^3} \sum_i \Delta_i^2 t_i^2$$

Combining this with (D33), we have (D31) for $m = 1$.

Case 2: Blocking occurs. For any ϕ, we can use (27) to lower bound a_{ik} by

$$a_{ik} \ge \frac{\partial A^f(f)}{\partial f_{ik}} + \frac{\partial A^\phi(\phi)}{\partial R_k} - \frac{\partial A^\phi(\phi)}{\partial R_i} \tag{D34}$$

$$\Delta_{ik} t_i \ge \min \left\{ \phi_{ik} t_i, \eta \left[\frac{\partial A^f(f)}{\partial f_{ik}} + \frac{\partial A^\phi(\phi)}{\partial R_k} - \frac{\partial A^\phi(\phi)}{\partial R_i} \right] \right\} \tag{D35}$$

The lower bounds above are continuous functions of ϕ. Since blocking occurs in ϕ, there is some i, k such that both

$$\frac{\partial A^\phi(\phi)}{\partial R_k} - \frac{\partial A^\phi(\phi)}{\partial R_i} \ge 0 \tag{D36}$$

and

$$\phi_{ik} t_i \ge \eta \left[\frac{\partial A^f(f)}{\partial f_{ik}} + \frac{\partial A^\phi(\phi)}{\partial R_k} - \frac{\partial A^\phi(\phi)}{\partial R_i} \right] \tag{D37}$$

Combining (D35) to (D37)

$$\Delta_{ik} t_i \geq \eta \frac{\partial A^f(f)}{\partial f_{ik}} \tag{D38}$$

Since the right-hand side of (D35) is continuous in ϕ, there is a neighborhood of ϕ^* around ϕ for which

$$\Delta^*_{ik} t^*_i \geq \frac{\eta}{2} \frac{\partial A^f(f)}{\partial f_{ik}} \tag{D39}$$

Equation (D31), for $m = 1$, now follows in the same way as in case 1.

Case 3: $\Delta_{ik} t_i = 0$ for all i, k. Let Φ_3 be the set of ϕ for which $\Delta_{ik} t_i = 0$ for all i, k. Let $\phi^{(l)} = \Gamma^l(\phi)$ for the given ϕ and let $m \geq 2$ be the smallest integer such that $\phi^{(m-1)} \notin \Phi_3$. We first show that $m \leq |\mathcal{V}|$. Note first that for any $\phi \in \Phi_3$, Γ changes ϕ_{ik} only for i such that $t_i = 0$ and thus the node data rates t and link data rates f cannot change. $\partial A^\phi / \partial R_i$ can change, however, and as we shall see later, must change for some i if ϕ does not minimize A^ϕ.

Now consider $\phi^{(l)}$ ($0 \leq l \leq m-2$, where $\phi^{(0)}$ denotes the original ϕ). Since $\phi^{(l)} \in \Phi_3$, $\Delta^{(l)}_{ik} > 0$ implies that $t_i = 0$. From (33), $\phi^{(l)}_{ik} = \Delta^{(l)}_{ik}$ and $\phi^{(l+1)}_{ik} = 0$. For a given i, all $\phi^{(l)}_{ik}$ are reduced to 0 except for the k which minimizes $\frac{\partial A^f(f)}{\partial f_{ik}} + \frac{\partial A^\phi(\phi^{(l)})}{\partial R_k}$. Thus, using (27),

$$\frac{\partial A^\phi(\phi^{(l+1)})}{\partial R_i} = \min_k \left[\frac{\partial A^f(f)}{\partial f_{ik}} + \frac{\partial A^\phi(\phi^{(l)})}{\partial R_k} \right] \leq \frac{\partial A^\phi(\phi^{(l)})}{\partial R_i} \tag{D40}$$

Since this equation is satisfied for all l, $0 \leq l \leq m-2$, we see that $\partial A^\phi(\phi^{(l)})/\partial R_i$ can be reduced on iteration l only if $\partial A^\phi(\phi^{(l-1)})/\partial R_k$ is reduced on iteration $l-1$ for some k such that $\partial A^\phi(\phi^{(l-1)})/\partial R_k < \partial A^\phi(\phi^{(l)})/\partial R_i$. This reduction at node k however implies a reduction at some node k' of smaller differential cost at iteration $l-2$ and so forth. Since this sequence of differential costs is decreasing with decreasing l and since (from (D40)) the differential cost at a given node is nondecreasing with decreasing l, each node in the sequence must be distinct. Since there are n nodes other than the given destination available for such a sequence, the initial l in such a sequence satisfies $l \leq |\mathcal{V}| - 2$. On the other hand, if $\partial A^\phi(\phi^{(l)})/\partial R_i$ is unchanged for all i, we see from (D40) that $\phi^{(l)}$ satisfies the sufficient conditions to minimize A^ϕ and then ϕ also minimizes A^ϕ contrary to our hypothesis; thus we must have $m \leq |\mathcal{V}|$.

Now observe that the middle expression in (D40), for $l = 0$, is a continuous function of ϕ and consequently $\partial A^\phi(\phi^{(1)})/\partial R_i$ is a continuous function of ϕ for all i. It follows by induction that $\partial A^\phi(\phi^{(l)})/\partial R_i$ is a continuous function of ϕ for all i and for $l \leq m-1$. Finally $\phi^{(m-1)} \notin \Phi_3$, so it must satisfy the conditions of case 1 or 2; it will be observed that the analysis there apply equally to $\phi^{(m-1)}$ because of the continuity of $\partial A^\phi(\phi^{(m-1)})/\partial R_i$ as a function of ϕ. This completes the proof. ■

Our last lemma will be stated in greater generality than required since it is a global convergence theorem for algorithms that avoids the usual continuity constraint on the algorithm. (See Luenberger [23]) for a good discussion of global convergence).

Lemma 13.7: Let Φ be a compact region of Euclidean N space. Let Γ be a mapping from Φ into Φ and let A^ϕ be a continuous real valued function in Φ. Assume that $A^\phi(\Gamma(\phi)) \leq A^\phi(\phi)$ for all $\phi \in \Phi$. Let A^ϕ_{min} be the minimum of A^ϕ over Φ and let Φ_{min} be the set of $\phi \in \Phi$ such that $A^\phi(\phi) = A^\phi_{min}$. Assume that for every $\phi \in \Phi - \Phi_{min}$, there is an $\epsilon > 0$ and an integer $m \geq 1$ such that for all $\phi^* \in \Phi$ satisfying $|\phi - \phi^*| < \epsilon$, we have $A^\phi(\Gamma^m(\phi^*)) < A^\phi(\phi)$. Then for all $\phi \in \Phi$,

$$\lim_{m \to \infty} A^\phi(\Gamma^m(\phi)) = A^\phi_{min}. \tag{D41}$$

Proof: See [8]. ■

Proof of Theorem 6.4: Let Φ be the set of loop-free routing variable ϕ such that $A^\phi(\phi) \leq A_0$. We have verified that Γ maps loop-free routing variables into loop-free routing variables, and from Lemma 13.5, $A^\phi(\Gamma(\phi)) \leq A^\phi(\phi)$ for $\phi \in \Phi$. Thus Γ is mapping from Φ into Φ. It is obvious that Φ is bounded and easy to verify that any limit of loop-free variables with $A^\phi(\phi) \leq A_0$ is also loop-free with $A^\phi(\phi) \leq A_0$. Thus ϕ is compact. The final assumption of Lemma 13.7 is established by Lemma 13.6. Thus Lemma 13.7 asserts the conclusion of Theorem 6.4. ■